



Univerza v Mariboru

Fakulteta za energetiko

Journal of ENERGY TECHNOLOGY



Volume 5 / Issue 4

NOVEMBER 2012

www.fe.uni-mb.si/si/jet.html

JOURNAL OF ENERGY TECHNOLOGY



VOLUME 5 / Issue 4

Revija Journal of Energy Technology (JET) je indeksirana v naslednjih bazah: INSPEC[®], Cambridge Scientific Abstracts: Abstracts in New Technologies and Engineering (CSA ANTE), ProQuest's Technology Research Database.

The Journal of Energy Technology (JET) is indexed and abstracted in the following databases: INSPEC[®], Cambridge Scientific Abstracts: Abstracts in New Technologies and Engineering (CSA ANTE), ProQuest's Technology Research Database.

JOURNAL OF ENERGY TECHNOLOGY

Ustanovitelji / FOUNDERS

Fakulteta za energetiko, UNIVERZA V MARIBORU /
FACULTY OF ENERGY TECHNOLOGY, UNIVERSITY OF MARIBOR

Izdajatelj / PUBLISHER

Fakulteta za energetiko, UNIVERZA V MARIBORU /
FACULTY OF ENERGY TECHNOLOGY, UNIVERSITY OF MARIBOR

Izdajateljski svet / PUBLISHING COUNCIL

Zasl. prof. dr. Dali ĐONLAGIĆ,

Univerza v Mariboru, Slovenija, **predsednik** / University of Maribor, Slovenia, **President**

Prof. dr. Bruno CVIKL,

Univerza v Mariboru, Slovenija / University of Maribor, Slovenia

Prof. ddr. Denis ĐONLAGIĆ,

Univerza v Mariboru, Slovenija / University of Maribor, Slovenia

Prof. dr. Danilo FERETIĆ,

Sveučilište u Zagrebu, Hrvatska / University in Zagreb, Croatia

Prof. dr. Roman KLASINC,

Technische Universität Graz, Avstrija / Graz University Of Technology, Austria

Prof. dr. Alfred LEIPERTZ,

Universität Erlangen, Nemčija / University of Erlangen, Germany

Prof. dr. Milan MARČIČ,

Univerza v Mariboru, Slovenija / University of Maribor, Slovenia

Prof. dr. Branimir MATIJAŠEVIČ,

Sveučilište u Zagrebu, Hrvatska / University in Zagreb, Croatia

Prof. dr. Borut MAVKO,

Inštitut Jožef Stefan, Slovenija / Jozef Stefan Institute, Slovenia

Prof. dr. Greg NATERER,

University of Ontario, Kanada / University of Ontario, Canada

Prof. dr. Enrico NOBILE,

Università degli Studi di Trieste, Italia / University of Trieste, Italy

Prof. dr. Iztok POTRČ,

Univerza v Mariboru, Slovenija / University of Maribor, Slovenia

Prof. dr. Andrej PREDIN,

Univerza v Mariboru, Slovenija / University of Maribor, Slovenia

Prof. dr. Jože VORŠIČ,

Univerza v Mariboru, Slovenija / University of Maribor, Slovenia

Prof. dr. Koichi WATANABE,

KEIO University, Japonska / KEIO University, Japan

Odgovorni urednik / EDITOR-IN-CHIEF

Andrej PREDIN

Uredniki / CO-EDITORS

Jurij AVSEC

Miralem HADŽISELIMOVIĆ
Gorazd HREN
Milan MARČIČ
Jože PIHLER
Iztok POTRČ
Janez USENIK
Peter VIRTič
Jože VORŠIČ

Uredniški odbor / EDITORIAL BOARD

Prof. dr. Jurij AVSEC,

Univerza v Mariboru, Slovenija / University of Maribor, Slovenia

Prof. ddr. Denis ĐONLAGIĆ,

Univerza v Mariboru, Slovenija / University of Maribor, Slovenia

Doc. dr. Željko HEDERIĆ,

Sveučilište Josipa Jurja Strossmayera u Osijeku, Hrvatska / Josip Juraj Strossmayer University
Osijek, Croatia

Doc. dr. Miralem HADŽISELIMOVIĆ,

Univerza v Mariboru, Slovenija / University of Maribor, Slovenia

Doc. dr. Gorazd HREN,

Univerza v Mariboru, Slovenija / University of Maribor, Slovenia

Prof. dr. Roman KLASINC,

Technische Universität Graz, Avstrija / Graz University Of Technology, Austria

dr. Ivan Aleksander KODELI,

Institut Jožef Stefan, Slovenija / Jožef Stefan Institute, Slovenia

Prof. dr. Jurij KROPE,

Univerza v Mariboru, Slovenija / University of Maribor, Slovenia

Prof. dr. Alfred LEIPERTZ,

Universität Erlangen, Nemčija / University of Erlangen, Germany

Prof. dr. Branimir MATIJAŠEVIĆ,

Sveučilište u Zagrebu, Hrvaška / University of Zagreb, Croatia

Prof. dr. Matej MENCINGER,

Univerza v Mariboru, Slovenija / University of Maribor, Slovenia

Prof. dr. Greg NATERER,

University of Ontario, Kanada / University of Ontario, Canada

Prof. dr. Enrico NOBILE,

Università degli Studi di Trieste, Italia / University of Trieste, Italy

Prof. dr. Iztok POTRČ,

Univerza v Mariboru, Slovenija / University of Maribor, Slovenia

Prof. dr. Andrej PREDIN,

Univerza v Mariboru, Slovenija / University of Maribor, Slovenia

Prof. dr. Aleksandar SALJNIKOV,

Univerza Beograd, Srbija / University of Beograd, Serbia

Prof. dr. Brane ŠIROK,

Univerza v Ljubljani, Slovenija / University of Ljubljana, Slovenia

Doc. dr. Andrej TRKOV,

Institut Jožef Stefan, Slovenija / Jožef Stefan Institute, Slovenia

Prof. ddr. Janez USENIK,

Univerza v Mariboru, Slovenija / University of Maribor, Slovenia

Doc. dr. Peter VIRTIČ,

Univerza v Mariboru, Slovenija / University of Maribor, Slovenia

Prof. dr. Jože VORŠIČ,

Univerza v Mariboru, Slovenija / University of Maribor, Slovenia

Prof. dr. Koichi WATANABE,

KEIO University, Japonska / KEIO University, Japan

Prof. dr. Mykhailo ZAGIRNYAK,

Kremenchuk Mykhailo Ostrohradskyyi National University, Ukrajina / Kremenchuk Mykhailo Ostrohradskyyi National University, Ukraine,

Doc. dr. Tomaž ŽAGAR,

Univerza v Mariboru, Slovenija / University of Maribor, Slovenia

Doc. dr. Franc ŽERDIN,

Univerza v Mariboru, Slovenija / University of Maribor, Slovenia

Tehniška podpora / TECHNICAL SUPPORT

Tamara BREČKO BOGOVČIČ,

Sonja NOVAK,

Janko OMERZU;

Izhajanje revije / PUBLISHING

Revija izhaja štirikrat letno v nakladi 150 izvodov. Članki so dostopni na spletni strani revije - www.fe.uni-mb.si/si/jet.html / The journal is published four times a year. Articles are available at the journal's home page - www.fe.uni-mb.si/si/jet.html.

Cena posameznega izvoda revije (brez DDV) / price per issue (VAT not included in price):
50,00 EUR

Informacije o naročninah / subscription information:

<http://www.fe.uni-mb.si/si/narocnine/index.php>

Lektoriranje / LANGUAGE EDITING

Terry T. JACKSON

Oblikovanje in tisk / DESIGN AND PRINT

Vizualne komunikacije comTEC d.o.o.

Oblikovanje revije in znaka revije / JOURNAL AND LOGO DESIGN

Andrej PREDIN

Revija JET je sofinancirana s strani Javne agencije za knjigo Republike Slovenije / The Journal of Energy Technology is co-financed by the Slovenian Book Agency.

Izgradnja plinovoda Južni tok se je začela

Južni tok se je s slovesnostjo, na kateri je bil navzoč tudi ruski predsednik Vladimir Putin, začel 7. 12. 2012 s simboličnim varjenjem prvih dveh cevi. Predsednik je poudaril pomembnost projekta za vse sodelujoče, med katerimi je tudi Slovenija. Med drugim je dejal, da bodo pri izvedbi projekta upoštevani najstrožji okoljski standardi, zato izgradnja plinovoda ne bo predstavljala nobene grožnje okolju.

V Sloveniji bo trasa plinovoda Južnega toka potekala deloma ob obstoječi trasi plinovoda. Južni tok bo v Sloveniji dolg približno 260 kilometrov, zato bosta predvidoma potrebni vsaj dve tlačni podpostaji. Seveda bo potrebno najprej pridobiti vso tehniško dokumentacijo, od okoljevarstvene presoje do državnega prostorskega načrta, kot osnove za izdajo gradbenega dovoljenja. Gradnja bo potekala v smeri od obstoječega plinovodnega priključka do Madžarske oz. do severa Italije. Izgradnja naj bi bila predvidoma dokončana do leta 2016, ko naj bi stekel prvi plin po našem delu plinovoda. Plinovodni del skozi Slovenijo naj bi financirala lastnika; država Slovenija preko družbe Južni tok Slovenija in Ruski Gazprom. Ocenjena vrednost Slovenskega dela plinovoda je približno milijarda evrov. Iz finančnega vidika gre večinoma za posojila, saj je slovenski del v višini petstotih milijonov za Slovenijo kar precejšen finančni zalogaj. Posojila naj bi se vračala iz prihodkov od tranzita plina čez Slovenijo, kar je ocenjeno na več kot sto milijonov evrov letno.

Na slovesnosti ob pričetku gradnje Južnega toka je bil prisoten tudi naš Minister za infrastrukturo in prostor, gospod Zvonko Černač, ki je povedal, da bodo prostorska dovoljenja v Sloveniji izdana pravočasno, da ne bo ovir pri izgradnji plinovoda. Poudaril je, da Južni tok pomeni dodatno energetska stabilnost Evrope in, da še večja energetska odvisnost Evrope od dobavitelja plina, Rusije, ni problematična. Trenutno namreč črpamo približno tretjino potreb po plinu v Sloveniji. Omenil je še, da projekt predstavlja dolgoročno in stabilno preskrbo, glede na povečane potrebe, ki se pričakujejo v prihodnjih dvajsetih letih (Delo, 8. 12. 2012).

Za Slovenijo pomeni gradnja Južnega toka vsekakor imenitno možnost za slovensko gospodarstvo, tako pri izvedbi del, kot tudi pri utrjevanju gospodarskega sodelovanja z Rusijo tudi v bodoče in na novih projektih. To bi vsekakor kazalo izkoristiti pri izhodu iz krize, ki je v Sloveniji žal v polnem razmahu, ne samo na gospodarskem, ampak tudi in predvsem na moralnem in socialnem področju, kar se kaže ob vse-slovenskih protestih civilnih iniciativ širom Slovenije.

Samo upamo lahko, da bo Slovenija za svoj razvoj in svetlejšo prihodnost znala izkoristiti dva velika energetska projekta, ob južnem toku še TEŠ 6.

Krško, december 2012

Andrej PREDIN

Construction of the pipeline – South Stream started

The President of Russia, Vladimir Putin, was present at the South Stream ceremony. It began on 7 December 2012 with the symbolic welding the first two tubes. The president explained the importance of the project for all involved, one of which is fortunately Slovenia. Among other things, he said that the project will be conducted according to the most stringent environmental standards, and that the construction of the pipeline will not constitute any threat to the environment.

In Slovenia, the route of the South Stream gas pipeline is partly on the existing route of a pipeline. South Stream will be around 260 kilometers long in Slovenia, and is expected to require at least two pressure substations. Of course, it will be necessary first to obtain all the technical documentation of the environmental assessment for the national spatial plan as a basis for a building permit. Construction will proceed in the direction of an existing pipeline connection to Hungary and the north of Italy. It is anticipated that the construction will be completed by 2016, when the first transfer of the gas to Slovenia's pipeline is expected. Part of the pipeline through Slovenia will be financially covered by the owners, the state of Slovenia, through the company South Stream Slovenia, and the Russian company Gazprom. The estimated value of the Slovenian part of the pipeline is around one billion euros. From the financial perspective, this is mainly for the loan, since the Slovenian part amounts to five hundred million euros, which is a significant amount for Slovenia. Loans are expected to be repaid by revenues from gas transit through Slovenia, estimated at more than a hundred million euros per year.

The ceremony marking the beginning of the construction of South Stream was also attended by our the Minister for Infrastructure and Spatial Planning, Zvonko Černač, who said that the planning permission will be issued in Slovenia in time, and that there will not be obstacles to the construction of the pipeline. He pointed out that South Stream adds energy stability of Europe and that even greater energy dependency of Europe from the gas supplier, Russia, is not a problem. In Slovenia, gas consumption currently represents only about a third of demand for gas in Slovenia. The project helps to ensure a long-term and stable supply, according to the increased demand, which is expected within the next twenty years (Delo, 12.8.2012).

For Slovenia, the construction of South Stream definitely represents a great economic opportunity, both in the execution of construction, as well as in strengthening future economic cooperation with Russia in new projects. This would certainly be beneficial in recovering from the economic crisis, which is unfortunately in full swing in Slovenia, not merely in the economy, but also and especially in the moral and social realms, as can be concluded from the frequent Slovenia-wide protests and civil initiatives.

We can only hope that Slovenia will be able to take advantages of two large energy projects, South Stream and the construction of the TEŠ 6 thermo-power plant, for its development and a brighter future.

Table of Contents /

Kazalo

Global testing of under-matched joints/

Globalno preizkušanje nizkotrdnostnih spojev

Zdravko Praunseis, Simon Marčič11

CFD investigation of the pressure distribution in centrifugal vortex impellers /

Numerična raziskava tlačne porazdelitve v radialnem vrtničnem rotorju črpalke

Tihomir Mihalić, Andrej Predin, Nenad Mustapić19

The influence of strength mismatching on the fracture properties of heterogeneous joints /

Vpliv trdnostne neenakosti na lomne lastnosti heterogenih spojev

Zdravko Praunseis, Sonja Novak, Jurij Avsec27

CAD mechanism simulations via web environments/

Simulacije mehanizmov CAD sistemov na spletu

Gorazd Hren, Ivan Žagar37

Numerical evaluation of the crack-driving force in heterogeneous regions /

Numerična določitev sile razvoja razpoke v heterogenih področjih

Zdravko Praunseis51

Instructions for authors59

GLOBAL TESTING OF UNDER-MATCHED JOINTS

GLOBALNO PREIZKUŠANJE NIZKOTRDNOSTNIH SPOJEV

Zdravko Praunseis[✉], Simon Marčič

Keywords: experiment, steel, under-matched joint

Abstract

The main aim of this experimental investigation was to determine whether the applied welding procedure for an under-matched welded joint with a soft root layer is appropriate for commercially available high strength low-alloyed steel. This steel usually requires preheating if a matching or overmatching weld consumable is used, which is not only expensive, but also needs a carefully designed and strictly followed welding procedure.

Povzetek

Glavna vsebina eksperimentalne raziskave je v določitvi optimalne tehnologije varjenja za nizkotrdnostni zvarni spoj z mehkim korenem glede na uporabo komercialnega visokotrdnostnega nizko legiranega jekla. Obravnavano jeklo pogostokrat zahteva uporabo predgrevanja v primeru uporabe enakotrdnostnih ali visokotrdnostnih dodatnih materialov za varjenje, kar pomeni visoke stroške proizvodnje in hkrati natančno določeno in vodeno tehnologijo varjenja.

[✉] Corresponding author: Zdravko Praunseis, PhD, Faculty of Energy Technology, University of Maribor, Tel.: +386 31 743 753, Fax: +386 7 620 2222, Mailing address: Hočevarjev trg 1, Krško, Slovenia, E-mail address: zdravko.praunseis@uni-mb.si

1 INTRODUCTION

High strength low-alloyed steel (HSLA), grade HT 80, quenched and tempered (Q + T), has been chosen for this investigation. This type of steel is used for high pressure pipelines, pressure vessels, bridges, various welded structures, including heavy ones (vehicles, storage tanks, auto cranes, etc.). Different mechanical properties of such steel can be obtained with different temperatures (600 °C–680 °C) during the tempering process, [1]. After the tempering process, the steel microstructure is bainitic, which guaranties its high strength and toughness (more than 130J at -50 °C). The steel is deformable in the hot state, in the temperature range 870 °C–970 °C. The time during which the steel is exposed to hot deformation temperatures is a function of thickness, but should be as short as possible. After hot deformation, the (Q + T) procedure should be performed again. Long heating in the two-phase range is not allowed, i.e. in the temperature range 720 °C–850 °C, since the yield strength will be reduced. The cooling after hot deformation is normally done in air. Stress relief heat treatment for this type of steel is not recommended, because of toughness reduction, especially for welded joints. If stress relief is needed due to the structure itself, then it is performed in the temperature region of 550 °C–600 °C only after a successful weldability test. After annealing, the steel is cooled in the furnace in a manner that depends on the structural requirements. The heating time is calculated from the plate thickness; it should not be shorter than 30 minutes.

The welded joints of this steel are sensitive to cold cracking, so the base material preheating [1–4] and drying of the covered electrodes is needed (350 °C/1 h), in order to reduce the weld's hydrogen to the greatest degree possible. Because of grain growth, this steel should be multi-pass welded with low input energy ($Q \approx 15\text{--}20$ kJ/cm). Preheating has beneficial effects, but post-weld heat treatment reduces the toughness and mechanical properties of the welded joint, so only post-heating up to 200 °C/1h should be used. A controlled cooling of all passes (inter-pass temperature) is needed.

For producing the under-matched weld, two different tubular wires were used; they are specially suitable for welding with mixture gas shielding (Fluxo Cored Arc Welding process-FCAW), primarily 80% Ar + 20% CO₂.

The aim of the global experimental testing of under-matched welded joints was to determine the proper welding procedure for a welded joint with a soft root layer.

2 WELDING PROCEDURE

The samples were completely fabricated and welded in the welding laboratory of Steelworks Jesenice. Welding was done on samples (500 × 250 × 40 mm) with an X-shaped groove (Fig.1).

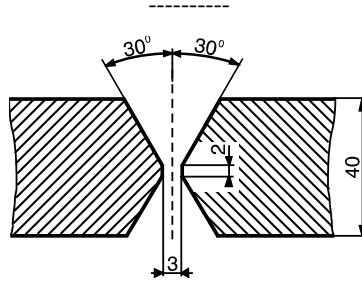


Figure 1: X-weld groove shape

Using the chosen welding procedure (Tab. 1), two different types of multi-pass butt X welds were made using the FCAW process with mixture gas shielding (80% Ar + 20% CO₂), i.e. an under-matched joint with homogeneous weld metal and a welded joint with a soft root layer (heterogeneous weld metal). The under-matched joint with the homogeneous weld metal (Fig. 2) was made with preheating and post-heating of the base material, entirely with the same consumable (WELTEC B 575 wire).

Table 1: Welding procedure for under-matched joint with homogeneous and heterogeneous weld metals

Under-matched weld joint	Homogeneous		Heterogeneous	
	root	cap	soft root	cap
Weld metal				
Consumable (tubular wire - $\phi 1.2$)	WELTEC B575	WELTEC B575	WELTEC B370	WELTEC B575
Preheating temperature, °C/2h	120	/	/	/
Heat input, Q(kJ/cm)	16.5	16–23	10.1	16–23
Calculated $\Delta t_{8/5,s}$	9.5	10.7	7.1	10.3
Measured $\Delta t_{8/5,s}$	8.9	9.2	6.7	8.6
Interpass temp., °C/2h	135	135	50	135
Preheating temp., °C/2h	/	200	/	/
Number of passes	2	14	2 (4)	16 (15)

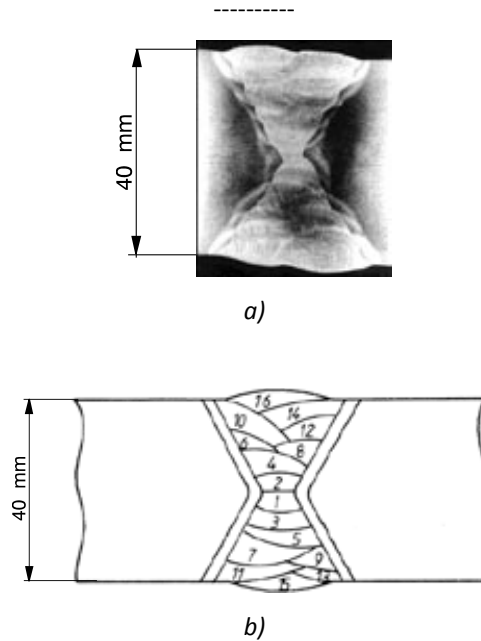


Figure 2: Cross-section of multi-pass under-matched joint with homogeneous weld metal a) and position - welding sequence of passes b)

The under-matched joint with the heterogeneous weld was made in order to avoid preheating the base material and to prevent cold cracking. For this purpose, a softer consumable was used for the root passes, the WELTEC B 370 wire with an expected mismatch factor of $M = 0.56$, while the WELTEC B 575 wire with an expected mismatch factor of $M = 0.76$ was used for filler passes (weld filler metal).

3 GLOBAL BEND TESTING OF WELDED JOINTS

For global bend testing of homogeneous and heterogeneous under-matched weld joints, side (Fig. 3) and cap (Fig. 4) flat specimens were taken from the welded joints. Bend testing was done in accordance with standard DIN 50121 at room temperature 20 °C.

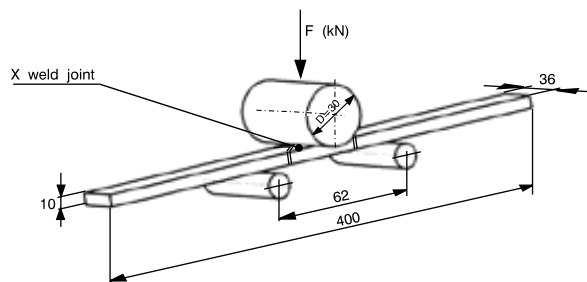


Figure 3: Shape and dimensions of side flat specimen and a mode of specimen bending

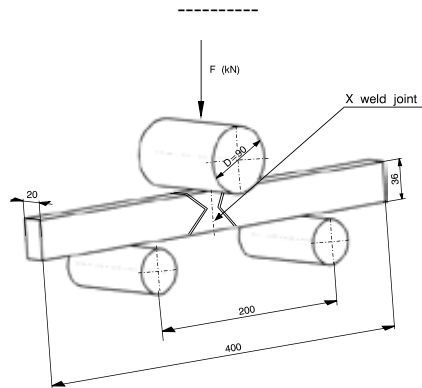


Figure 4: Shape and dimensions of cap flat specimen and a mode of specimen bending

In the real welded joint, the existence of weld defects cannot be excluded (e.g. lack of fusion, slag inclusions, etc.). Therefore, by using the standard bending of a welded joint, the 'homogeneity' of under-matched weld metal and heat-affected zone (HAZ) can be examined. Specimens were first bent to the angle where the initial crack in the welded joint appeared (initiation due to defect presence); they were the fractured, i.e. the crack was opened at the final angle. These bending angles are given in Tab. 3.

Table 3: Results of measured initial (α_0) and final (α_p) bending angles during under matched weld joint bending

Specimen			Bending angle		
			initial angle (α_0)	final angle (α_p)	
Cap specimen	Homogeneous weld metal	M1	15°	148°	
		M2	54°	148°	
	Heterogeneous weld metal	2 passes	D1	6°	18°
			D2	18°	82°
		4 passes	E3	44°	65°
			E4	14°	26°
Side specimen	Homogeneous weld metal	M1	180°*	-	
		M2	50°	-	
		M2	12°	-	
	Heterogeneous weld metal	2 passes	D1	10°	-
			D2	12°	-
		4 passes	E3	34°	-
			E4	18°	-

* - bending up to angle 180°

The weld joint appearance at crack initiation and at fracture is shown in Fig. 5 and Fig. 6.

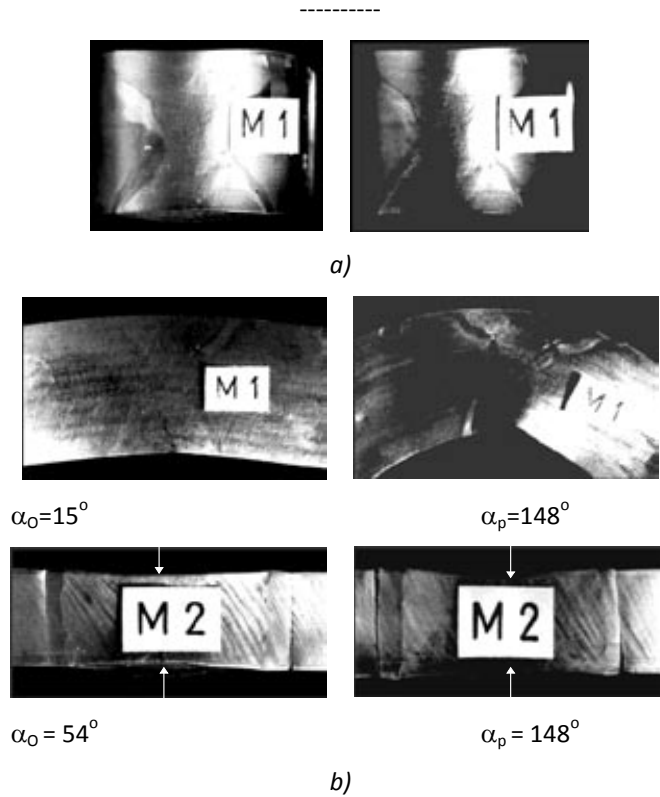


Figure 5: The appearance of homogeneous under-matched weld joint during side a) and cap b) specimen bending

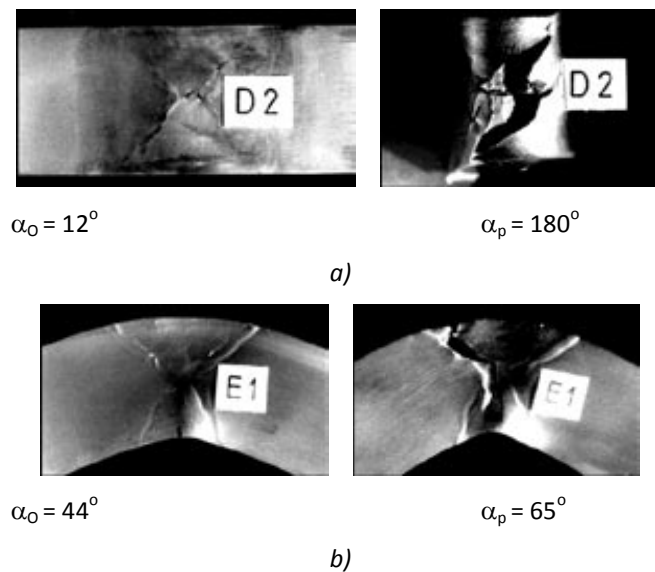


Figure 6: The appearance of heterogeneous under-matched weld joint during side a) and cap b) specimen bending

By reviewing the results, [1], of flat specimens in regard to the global values of strength mismatch factors M , it is clear that the under-matched heterogeneous weld joints attained approximately 10% lower strength properties than the homogeneous weld joints. The flat specimens with homogeneous weld joints did not fail in the weld metal, but rather in the base material, because of the higher strength of the overmatched root weld metal and the somewhat lower strength of the under-matched weld filler metal, providing an overall higher strength of the weld, as was already concluded during the discussion of local factors M for homogeneous under-matched weld joints. Consequently, the yield strength was on average reached first in the base material, causing plastic strains and final failure there. In such welded joints, the effect of different regions on its tensile properties emerged, not only as a consequence of the weld metal and base material interaction, but also as a consequence of interactions between the overmatched root weld metal and weld filler metal, and of the base material and root weld metal, which is the region in welded joints with the highest yield strength. In order to prove this statement, the specimen M2 (Fig. 5.) taken from weld filler metal (Fig. 6) was tested in bending, showing side contraction of the weaker weld metal.

In the heterogeneous weld joints, the yield strength was first reached in the soft root layer. Because the yield strength of the soft root layer was lower than in other welded joint regions, including the base material, material de-cohesion due to the high plastic deformation started there. Fracture propagation toward the weld filler metal followed afterwards (maximum fracture force was reached first in the root layer), which was also proved by the diagonal fracture of the flat specimen, [2].

The results (Tab. 3) for measured initial - α_0 (first crack initiation) and final - α_p (weldment fracture) bending angles in the cap (Fig. 5) and side (Fig. 6) flat specimens have shown lower values for heterogeneous welds than for the homogeneous ones, because the crack was initiated in the soft root weld metal (Fig. 6), where it also caused the final fracture.

4 CONCLUSIONS

The lower strength of soft root layer means lower global strength of under-matched heterogeneous welded joints if compared to under-matched homogeneous welded joints without soft root layers.

The selection of soft tough weld consumable (wire) does not guarantee a tough root layer in the under-matched welds, since the root weld metal alloying from the base material depends on the consumable and the welding procedure. Improper selection of weld consumables and the thermal effects of subsequent passes on soft root layer built up can modify the microstructure of all-weld metal (wire) and with that lower its toughness.

A welding procedure without preheating of HSLA steel aimed at producing under-matched joints with the soft root layer presents a technological challenge for modern welded structure fabrication. Such a procedure should achieve higher toughness in its soft root layer than in the filler and cap passes, and in its HAZ.

Acknowledgements

The authors wish to acknowledge the financial support of the Slovenian Foundation of Science and Technology and the Japanese Promotion of Science.

References

- [1] **Praunseis, Z.:** *The influence of Strength Under-matched Weld Metal containing Heterogeneous Regions on Fracture Properties of HSLA Steel Weld Joint* (Dissertation in English). Faculty of Mechanical Engineering, University of Maribor, Slovenia, 1998
- [2] **Praunseis, Z., Toyoda, M., Sundararajan, T.:** *Fracture behaviours of fracture toughness testing specimens with metallurgical heterogeneity along crack front*. Steel res., Sep. 2000, 71, no 9,
- [3] **Praunseis, Z., Sundararajan, T., Toyoda, M., Ohata, M.:** *The influence of soft root on fracture behaviors of high-strength, low-alloyed (HSLA) steel weldments*. Mater. manuf. process., 2001, vol. 16, 2
- [4] **Sundararajan, T., Praunseis, Z.:** *The effect of nitrogen-ion implantation on the corrosion resistance of titanium in comparison with oxygen- and argon-ion implantations*. Mater. tehnol., 2004, vol. 38, no. 1/2.

CFD INVESTIGATION OF THE PRESSURE DISTRIBUTION IN CENTRIFUGAL VORTEX IMPELLERS

NUMERIČNA RAZISKAVA TLAČNE PORAZDELITVE V RADIALNEM VRTINČNEM ROTORJU ČRPALKE

Tihomir Mihalić[✉], Andrej Predin, Nenad Mustapić

Keywords: centrifugal vortex impeller, computational fluid dynamics, cavities.

Abstract

A Computational Fluids Dynamics (CFD) analysis of the pressure fields in a centrifugal vortex impeller was undertaken in this paper. The aim was to increase pressure distribution along the impeller blades to determine whether a vortex impeller added to the centrifugal impeller can delay the start of cavitation.

The calculating domain was mesh by finite control volumes, and equations were solved with ANSYS FLUENT 14. Furthermore, the measurement results were used as experimental validation of numerical simulations. This validation was done by taking pressure measurements at some locations in experimental models, and comparing them with those obtained with CFD simulations.

It was shown that the centrifugal vortex impeller generates higher pressure in critical areas along the blades than the centrifugal impeller does for the same head.

[✉] Corresponding author: Tihomir Mihalić, PhD., Faculty of Mechanical Engineering and Naval Architecture, Zagreb, Tel.: +385 98 686 072, Fax: +385 1 616 8127, Mailing address: I.Lučića 5, Zagreb, Croatia
E-mail address: tihomir.mihalic@fsb.hr

Povzetek

V prispevku je podana analiza tlačnih polj v radialnem vrtničnem rotorju, izvedena na osnovi računalniške dinamike tekočin (CFD). Bistvo prispevka je v določitvi tlačne porazdelitve vzdolž rotorskih lopatic, ki naj prikaže koliko prispeva razvit rotorjev vrtinec k zakasnitvi formiranja prvih kavitacijskih zarodnih mest (kavern).

Celotno zamreženje računske domene, kot tudi rešitve sistema enačb je izvedeno z ANSYS FLUENT 14 programom. Rezultati izračuna so validirani ob pomoči eksperimentalno izmerjenih podatkov. Primerjani so izmerjeni tlaki na posameznih lokacijah, identičnih pri meritvah in v izračunih.

Z numeričnimi rezultati je prikazano, da radialni rotor z razvitim vrtincem generira višje tlake na kavitacijsko kritičnih mestih vzdolž rotorske lopatice radialne črpalke pri doseženi isti črpalni višini.

1 INTRODUCTION

Improving the operating characteristics of centrifugal pumps by adding a vortex rotor to the centrifugal rotor was determined by Mihalić et al., [1]. In this derived centrifugal vortex rotor, the energy of the induced vortices at the vortex rim is added to fluid energy gained in the centrifugal rotor, Fig. 1.



Figure 1: Centrifugal vortex rotor

Zhejiang Sci-Tech University, [5], has performed experimental studies on vortex centrifugal pumps, in which the centrifugal and vortex rotor are on the same shaft, but separated, Fig. 2. From their results, it can be seen that this centrifugal vortex pump has improved supply, and that the flow cuts off with the 15% higher gas content in the liquid, compared to the centrifugal pump.

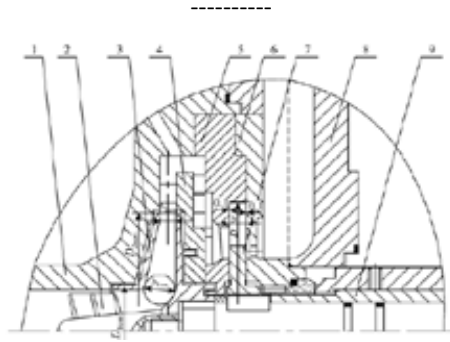


Figure 2: Centrifugal vortex pump stage with separated centrifugal and vortex rotor; 1-inlet casing; 2-inducer; 3-centrifugal impeller; 4-interstage diffuser; 5-suction; 6-discharge;7-vortex impeller; 8-outlet casing; 9-shaft sleeve

During this research, physical models of the centrifugal pump and centrifugal vortex pump were made, which corresponded to numerical models. An original experimental bed was developed. In that experimental procedure, special care was taken with the flow measurements. The reason for this is in the fact that the flow measurements had the greatest influence on the overall measurement uncertainty. However, flow measurements were the most demanding with regards to experiment design and in taking the measurement readings.

The objectives of this research were to confirm whether or not a centrifugal vortex impeller can demonstrate some operating benefits regarding cavitation.

2 NUMERICAL MODEL OF CENTRIFUGAL VORTEX PUMP

Numerical simulations of unsteady flow included the entire centrifugal and centrifugal vortex pump stage, including suction and discharge pipes, Fig. 3.

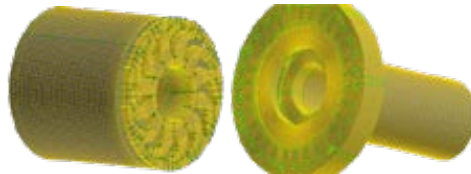


Figure 3: CV mesh of centrifugal vortex pump stage. On the left is the meshed stator with the outlet. On the right is the meshed rotor with inlet pipe.



Figure 4: CV mesh of stator (left) and rotor (right).

The entire continuum was meshed with three different meshes of control volumes, consisting of: 962,159 CV (longest edge 0.5 mm), 1,864,399 CV (longest 0.4 mm) and 3,340,658 CV (longest edge 0.3 mm).

After research for a suitable time step with respect to convergence it was set to 8×10^{-5} s, by which rotor is turned by 1.5° . With a selected time step, the mean Courant number (CFL) was 0.5179. As a working fluid, water of standard properties at 25°C was used.

Turbulence was modelled using a hybrid model - detached eddy simulations (DES) after it was verified, [6] and [7].

In the CFD simulations of the cavitations, a multi-phase model called "Mixture" was used. It was used to model water - water vapour content. The formation of water vapour (cavitation) was modelled by the Schnerr-Sauer model according to [14–16].

3 RESEARCH RESULTS

3.1 Analysis of the pressure field in centrifugal vortex and centrifugal pump stage

For the pressure field analysis, rotors were sectioned by the perpendicular plane to the rotation axis, at exactly half the width of the centrifugal blades, [13].

Comparing the suction Area A in Fig. 5, it can be concluded that the centrifugal pump creates a much wider suction area with the same head and supply.

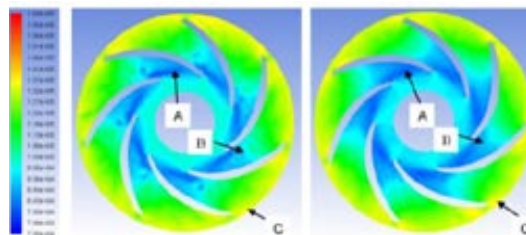


Figure 5: Pressure field in centrifugal vortex (left) and centrifugal (right) pump stage; $k_L = 0$

The area of the lower pressure at the centrifugal vortex pump collapses more quickly with the shredding of vortices, Area B, Fig. 5, while this transition in the centrifugal pump is more continuous. The only logical conclusion is that the vortex rim affects the suction area by accelerating this transition.

The attenuating flow, $k_L = 5$ (the pressure fields and the form of suction area) for both pumps becomes similar, Fig. 6. It can be seen that the point of the lowest pressure (highest under-pressure), in both pumps, is located just below the leading edge of the concave side of the rotor blades (Point A).

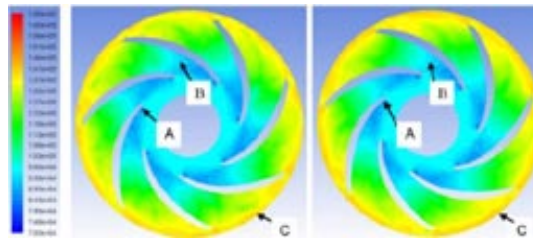


Figure 6: Pressure field in centrifugal vortex (left) and centrifugal (right) pump stage; $k_L = 5$

This suction pressure (Point A) is lower in the centrifugal pump. Unlike the previous working regime of the centrifugal vortex pump, here the pressure increases gradually over the isobars, which are perpendicular to the concave side of the rotor blade (Point B).

Fig. 7 shows the pressure fields in the pumps when $k_L = 60$. It can be seen that the suction area at both the pumps quickly collapses.

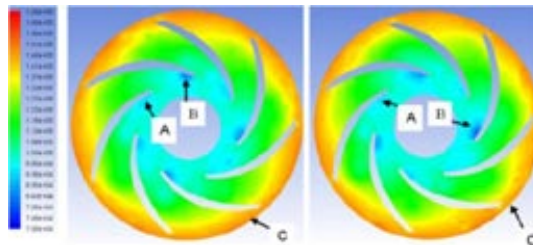


Figure 7: Pressure field in centrifugal vortex (left) and centrifugal (right) pump stage; $k_L = 60$

This suction area (Point A and Point B) is more concentrated at the centrifugal vortex pump. It can be at the concave side of the impeller blades, but also away from concave side, somewhere in the middle of the flow. Integrating static and dynamic pressure at the perimeter of the rotor in this regime means that the centrifugal pump realizes higher static pressure but lower dynamic pressure than the centrifugal vortex pump.

Fig. 8 shows the pressure field in pumps at the final attenuation of the flow (fully closed valve at the pump discharge) $k_L = 300$. The suction area at both pumps quickly transitions to higher pressure. The lowest pressure point (Point A and Point B) in the centrifugal vortex pump is in front of the leading edge of the blades and away from the blades in the fluid.

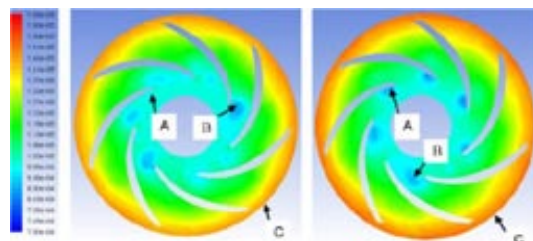


Figure 8: Pressure field in centrifugal vortex (left) and centrifugal (right) pump stage; $k_L = 300$

This lowest pressure point in the centrifugal pump is still on the concave side of the blades.

From the analysis of the lowest pressure in the pumps working at different regimes, the diagram shown on Fig. 9 can be derived.

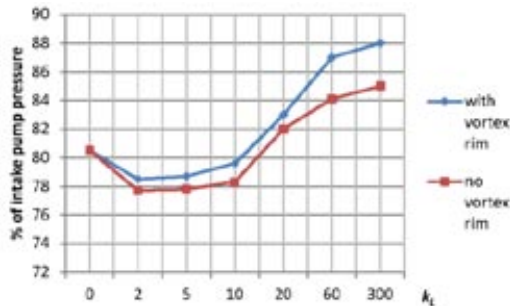


Figure 9: Lowest pressure in the pumps rotors

A centrifugal vortex pump generates higher suction pressure (smaller under-pressure) while giving higher head and supply. The biggest difference of these suction pressures occurs at the end of the working regime at the full flow attenuation. From the loss coefficient $k_L = 20$ towards $k_L = 300$, a centrifugal rotor of the centrifugal vortex pump starts to lag in its work capacity and the vortex rim starts to compensate, allowing it to establish a smaller under-pressure.

How low suction pressure can be at the centrifugal vortex pump is determined by the vortex rim. The maximum static overpressure generated by the vortex rim at its outer diameter is the static overpressure, which the centrifugal rotor must generate at the same diameter because the vortex rim is downstream from the centrifugal rotor.

At higher angular velocities, the vortex rim creates increasingly coherent structures, so an increasingly dynamic pressure is achieved, producing progressively lower static overpressure. To preserve the balance, the centrifugal rotor must follow these tendencies imposed by the vortex rim. In order for that to occur, the centrifugal rotor also needs to generate lower static overpressure at its outer diameter; this requires a smaller under-pressure at the pump intake.

The vortex rim acts as the regulator for the centrifuge rotor of the centrifugal vortex pump. This property is important for the stability of the pump cavitation.

3.2 CFD simulation of cavitation

To verify that the delay in vortex rim cavitation occurs in the centrifugal vortex pump, a detailed CFD study was carried out at a flow attenuation of $k_L = 60$. Simulations were carried out by varying angular velocities from 5500 min^{-1} up to 10000 min^{-1} at increments of 500 min^{-1} .

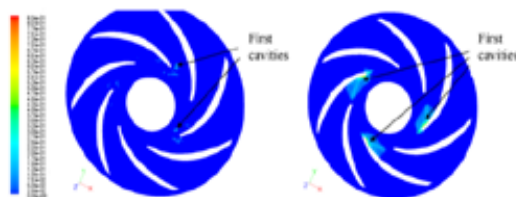


Figure 10: Occurrence of first cavities in the centrifugal vortex pump (left, $n = 9000 \text{ min}^{-1}$) and centrifugal pump (right, $n = 7500 \text{ min}^{-1}$)

Fig. 10 shows the occurrence of the first cavitation caverns with a share of water vapour in the water. It was discovered that the first cavities are formed in the centrifugal vortex pump at 9000 min⁻¹ and in the centrifugal pump at 7500 min⁻¹. It can be concluded that the vortex rim delays cavitation for about 20% of the centrifugal pump angular velocity.

Furthermore, it seems that cavitation in the centrifugal vortex pump has a tendency to form in the fluid away from its rotor blades, which is even more beneficial. It can be concluded that the blades at the inlet of the centrifugal vortex pump are protected from cavitation erosion by the vortex rim.

4 CONCLUSION

It has been shown that the vortex rim regulates suction under-pressure in the centrifugal rotor. This suction under-pressure is smaller than in a similar centrifugal pump providing a delay of cavitation and hence increasing the working stability. CFD simulations of the cavitation have shown that at the same working regime (installation characteristic), the centrifugal pump starts to cavitate at a 20% lower angular velocity than the centrifugal vortex pump. It has been shown that cavitation at the centrifugal vortex pump originates in the fluid, not on blades.

It is assumed that the centrifugal vortex pump will have better performances than centrifugal pumps when the working fluid is multiphase. This must be verified in further research, but the blades of the vortex rim should have a positive effect if there are gas bubbles or even sludge in the working fluid.

It can be concluded that centrifugal vortex pumps have some key operating benefits that can be decisive factors in their development and usage. These benefits manifest in extreme working conditions (low flow, high system resistance), so if head and cavitation characteristics are more important factors than energy consumption, it is reasonable to use a centrifugal vortex pump instead of a plain centrifugal one.

References

- [1] **T. Mihalić, Z. Guzović, S. Sviderek** (2011), *Improving centrifugal pump by adding vortex rotor*, Journal of Energy Technology, Slovenia, pp. 11–20.
- [2] **Z. Zuchao, X. Peng, O. Guofu, C. Baoling, L. Yi** (2008). *Design and experimental analyses of small-flow high head centrifugal-vortex pump for gas-liquid two phase mixture*. Chinese Journal of Chemical Engineering, 16: 528–534
- [3] **P.R. Spalart** (2009). *Detached-eddy simulation*. Annual Review of Fluid Mechanics, Vol. 41(1), pp.181–202
- [4] **A. Travin, M. Shur, M. Strelets, P.R. Spalart** (1999). *Detached eddy simulations past a circular cylinder*. Flow, Turbulence and Combustion, Vol. 63, pp.293–313.
- [5] **K.A. Kaupert, T. Staubli** (2003). *The Unsteady Pressure Flow in a High Specific Speed Centrifugal Pump Impeller – Part II: Large Eddy Simulations*. J. Fluids Eng. 125, Vol. 73
- [6] Fluent Inc (2008). *Fluent 12 user guide*.
- [7] **R.W. Dochterman**, General Electric Company (1974), Centrifugal-vortex pump, *United States Patent 3,936,240*, USA.

-
- [8] **V.S. Lobanoff, R.R. Ross** (1992), *Centrifugal pumps – Design & Application, 2nd edition*, Butterworth-Heinemann, USA.
 - [9] **J. F. Gülich** (2008), *Centrifugal Pumps*, Springer Berlin Heidelberg New York.
 - [10] **A. Predin** (2000). *Črpalke in ventilatorji*. Univerzitetna knjižnica Maribor, Slovenija, Maribor
 - [11] **M. Manninen, V. Taivassalo and S. Kallio** (1996). *On the mixture model for multiphase flow*. VTT Publications 288, Technical Research Centre of Finland.
 - [12] **G.H. Schnerr and J. Sauer** (2001). *Physical and Numerical Modeling of Unsteady Cavitation Dynamics*. In Fourth International Conference on Multiphase Flow, New Orleans, USA.

Nomenclature

H	Head
Q	flow rate
n	angular velocity

THE INFLUENCE OF STRENGTH MISMATCHING ON THE FRACTURE PROPERTIES OF HETEROGENEOUS JOINTS

VPLIV TRDNOSTNE NEENAKOSTI NA LOMNE LASTNOSTI HETEROGENIH SPOJEV

Zdravko Praunseis[✉], Sonja Novak, Jurij Avsec

Keywords: strength mismatching, fracture properties, steel joints

Abstract

The differences in mechanical properties among different weld regions affect the strain distribution around the crack tip during fracture toughness tests and consequently influence the fracture toughness values. This paper demonstrates that both strength and toughness affect the fracture behaviour of such complex weldments. High toughness of weld metal is necessary to enable local plastic deformation and to prevent brittle fractures. It is of the utmost importance not to exclude the possibility of plane faults and the appearance local brittle zones in steel welded joints, which can cause failure in heat affected zones and also in weld metal.

Povzetek

Razlike v mehanskih lastnostih vzdolž različnih področjih v materialu zvara vplivajo na porazdelitev napetosti na konici razpoke med lomnomehanskim preizkusom in posledično tudi na vrednosti lomne žilavosti. Ugotovitev pove, da dejansko tako trdnost kot žilavost kontrolirata lomno obnašanje kompleksnih zvarov. Visoka žilavost zvara je nujna za zadrževanje lokalnih plastičnih deformacij in s tem preprečitev krhkega loma. Zaradi tega je pomembno, da ne izključimo možnosti nastanka ploskovnih napak in lokalnih krhkih področij v zvarnih spojih, ki lahko povzročijo lom v toplotno vplivanem področju in zvaru.

[✉] Corresponding author: Zdravko Praunseis, PhD, Faculty of Energy Technology, University of Maribor, Tel.: +386 31 743 753, Fax: +386 7 620 2222, Mailing address: Hočevarjev trg 1, Krško, Slovenia, E-mail address: zdravko.praunseis@uni-mb.si

1 INTRODUCTION

In welded joints made of high-strength, low-alloyed (HSLA) steels, there is often a mismatch of strength between the weld metal (WM), the base material (BM) and the heat-affected-zone (HAZ), [1–4]. When the yield point is lower in the WM in comparison to the BM, the welded joint is under-matched. The strength mismatch factor (M) is defined as the ratio of WM to BM yield strengths, so that $M < 1$ defines an under-matched welded joint. Using the strength mismatch factor, one can describe the strength heterogeneity in every point of a welded joint.

Regarding HSLA steels' weldability, it is more economical to produce under-matched welded joints, [2]. Attention should be given to the level of strength mismatching that should be sufficient to provide sufficient toughness of the WM by using appropriate weld consumable (wire, electrode) and welding procedure, [3]. The basic concept of an under-matched welded joint with a plane crack is to have BM and HAZ in an elastic stress state, while the more ductile WM is plastically deformed. The question arises of whether the stability point of short cracks in an under-matched welded joint is reached or not.

The aim of this investigation is to systematically analyse the mechanical strength behaviour of multi-pass under-matched welded joints, made with and without soft root layers. The soft root layer was made with softer (lower yield strength) electrodes (tubular wires) in order to prevent cold cracking and to enable lower preheat temperatures.

2 EXPERIMENTAL PROCEDURE

The under-matched joint with the heterogeneous weld (Fig. 1) was made in order to avoid preheating of the base material and to prevent cold cracking. For this purpose, a softer consumable was used for the root passes, the WELTEC B 370 wire with an expected mismatch factor of $M = 0.56$, while the WELTEC B 575 wire with an expected mismatch factor of $M = 0.76$ was used for filler passes (weld filler metal).

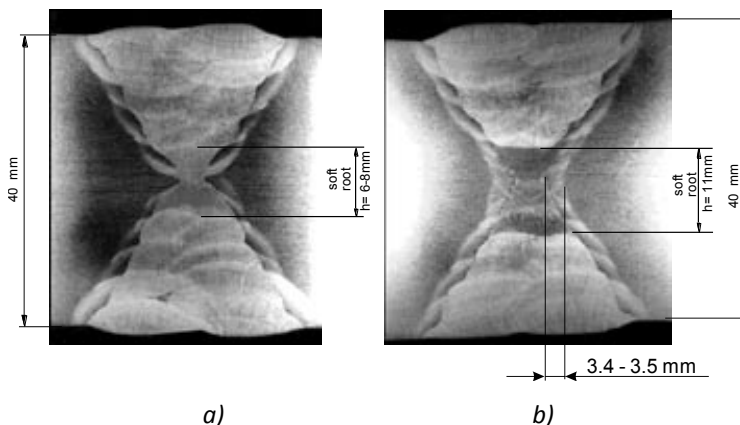


Figure 1: Cross-sections of multi-pass under-matched joints with heterogeneous weld with two passes a) and four passes b) soft root layer

The soft root layer was also welded with basic covered electrode (EVB 47 - ϕ 3.25). The diffusion hydrogen was measured after previous electrode drying (1h/400 °C). The measured value $H_D = 0.77$ ml/100 g represents a low H_D value for covered electrodes, which prevents cold cracking even for very low base material preheating temperatures, [1]. The soft root layer EVB 47 was welded in order to compare the mechanical properties with the properties of the root layer welded with WELTEC B 370 tubular wire (Fig. 2). The chemical composition and mechanical properties of the all-weld metal EVB 47, as well as mechanical and toughness properties of the soft under-matched root layer are given in Tab. 1b. The welding procedure for the soft root layer EVB 47 is given in Tab. 1a.

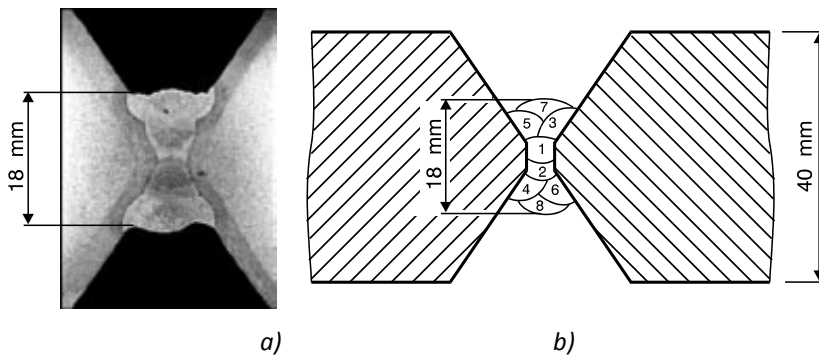


Figure 2: Cross-section of root layer welded with basic covered electrode EVB 47 - ϕ 3.25 a) and welding sequence b)

Table 1: Welding procedure a) and chemical composition and mechanical properties b) of soft root layer - EVB 47

Under-matched weld joint	Heterogeneous	
	root	cap
Weld metal	root	cap
Consumable (tubular wire ϕ 1.2)	EVB -47	/
Preheating temperature, °C/2h	/	/
Heat input, Q(kJ/cm)	5.6	/
Calculated $\Delta t_{8/5,s}$	6.2	/
Measured $\Delta t_{8/5,s}$	5.1	/
Inter-pass temp. °C/2h	50	/
Post-heating temp. °C/2h	/	/
Number of passes	8	/

a)

Designation	Rp (MPa)		Rm (MPa)		Elongation (%)		Charpy toughness (J)		Expected M		Achieved M
	C	Si	Mn	P	S	Cr	Ni	Mo	Cu	Al	
EVB - 47 all-WM	422		484		26.5		253,261,269 at -40 °C		0.60		
EVB - 47 soft root	493		554		25.9		63,75,57 at -10 °C		0.60		0.71
Chemical composition	C	Si	Mn	P	S	Cr	Ni	Mo	Cu	Al	
EVB - 47 all-WM	0.05	0.22	0.75	0.012	0.009	-	-	-	-	-	

b)

3 RESULTS AND DISCUSSION

In the under-matched joint with homogeneous and heterogeneous weld metals, besides the global strength mismatch between the weld metal and base material, there is also a local strength mismatch between the weld metal and HAZ, and root weld metal and weld filler metal (filler passes), which is more pronounced for a joint with the soft root layer. Local strength mismatching is especially pronounced in the thickness direction of the under-matched joints with homogeneous (Fig. 1a) and heterogeneous (Fig. 1b) weld metals, which has been determined by measurement of the micro-hardness (the distance between indents was 1 mm). To evaluate local strength mismatching between weld metal and HAZ, micro-hardness was measured in the weld filler metal and in the weld root of the under-matched joints with homogeneous and heterogeneous weld metals.

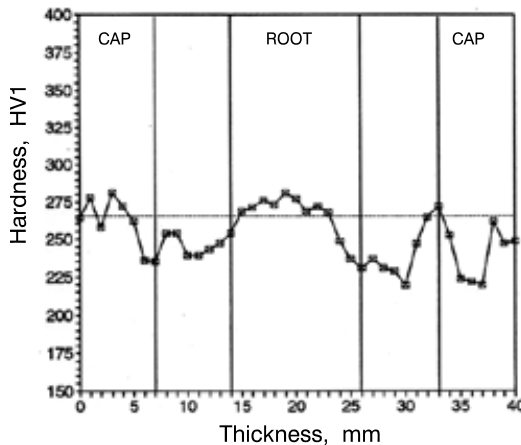


Figure 3: Micro-hardness values measured through the thickness direction of under-matched weld metal

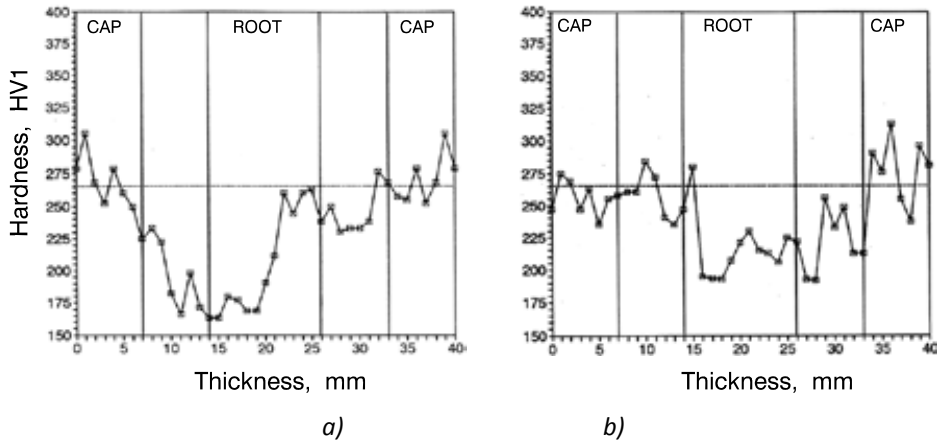


Figure 4: Micro-hardness values measured through the thickness direction of under-matched weld metal with two-pass a) and four-pass soft root layer b)

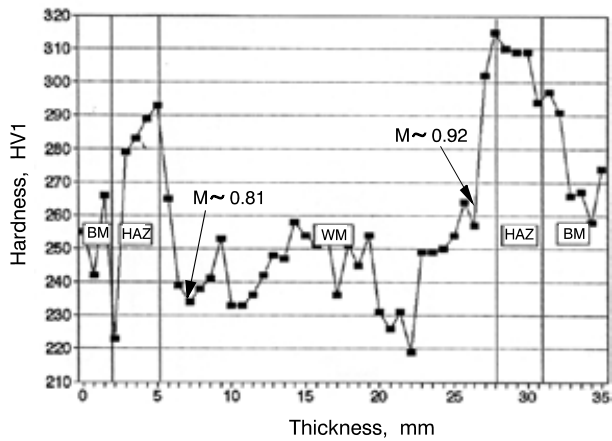


Figure 5: Micro-hardness distribution in the transverse direction of the under-matched homogeneous weld joint

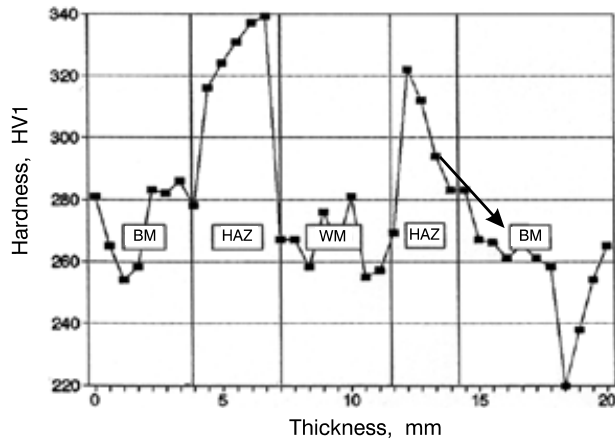


Figure 6: Micro-hardness distribution in the transverse direction of the root region of the under-matched homogeneous weld joint

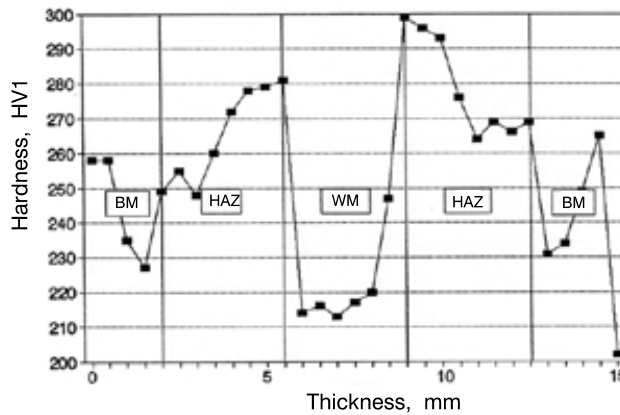


Figure 7: Micro-hardness distribution in the transverse direction of the root region of the under-matched heterogeneous weld joint

Strength heterogeneity of a welded joint is defined by the local mismatching factor ($M = R_{pweld}/R_{pbm}$). To evaluate the weld metal yield strength, the experimental correlation ($R_p = 3.15HV-168$) is often used, [1], employing measured HV.1 micro-hardness values in all joint points (Fig.3, Fig.4, Fig.5, Fig.6 and Fig.7). In this way, it is possible to roughly determine the strength mismatching factor M in every point of the welded joint. Its distribution in the thickness direction of the under-matched joints with homogeneous and heterogeneous weld metals is shown in Fig. 8 and 9.

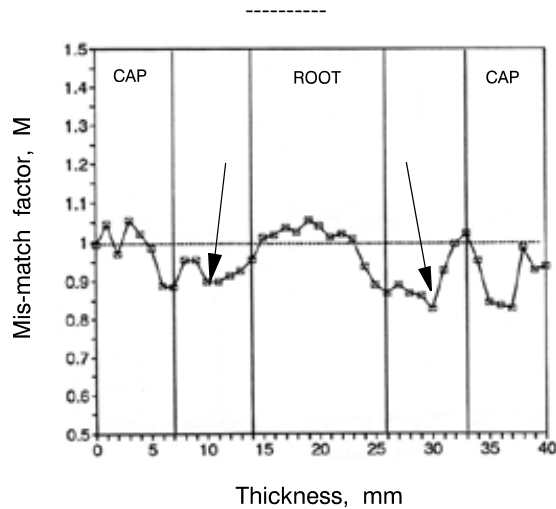


Figure 8: Distribution of the strength mismatching factor M across the thickness of multi-pass homogeneous under-matched weld

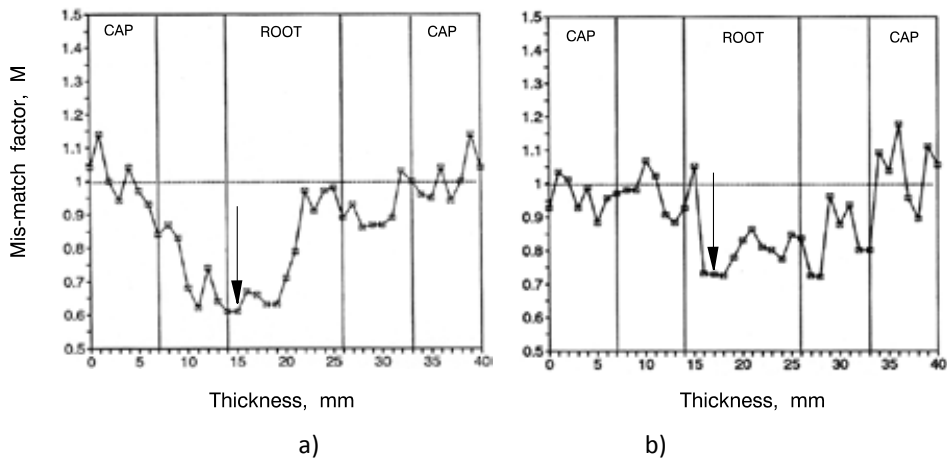


Figure 9: Distribution of the strength mismatch factor M across the thickness of the under-matched welded joints with two-pass a) and four-pass b) soft root layer

The expected mechanical properties of homogeneous and heterogeneous under-matched weld joints have not been attained in the weld filler metal (filler passes), or in the root weld metal, compared to mechanical properties of all-weld metal and real under-matched welded joints. The reason was the weld metal alloying with elements from the diluted base material.

The alloying effect was more pronounced in the root region than in the weld filler metal, and it was also the main reason for local strength mismatch appearing in thickness direction of homogeneous and heterogeneous welds. Different values of strength mismatch factor M

(calculated [1] from measured micro-hardness) through the thickness of homogeneous and heterogeneous weld metal (Fig. 8 and 9) indicate how complex the determination of the global M for real welded joints is. One of the reasons is the action of different alloying and dilution mechanisms during welding in the weld pool and, as a consequence of this effect, the change of weld metal hardening ability. The mismatch factors M in Fig. 8 and Fig. 9 and Tab. 1b can be compared, but one should consider that the mechanical properties given in Tab. 1b are valid only for those weld metal regions from which the specimens were taken, and thus cannot represent the strength mismatch accuracy of the whole welded joint. Having in mind the values of strength mismatch factors M in Tab. 1b, one can see that the homogeneous root weld metal is actually overmatched (Fig.8), which leads to strongly increased cold cracking susceptibility, whereas the weld filler metal has practically the same strength as the base material. This effect approves the concept of heterogeneous weld in an under-matched joint with a two-pass ($M = 0.8 \Rightarrow 20\%$ under-matching) or a four-pass ($M = 0.9 \Rightarrow 10\%$ under-matching) soft root layer in order to prevent cold cracking without preheating of the base material. Similar conclusions can be reached by analysing the distribution of factors M obtained from measured hardness (Fig.8 and Fig.9) and calculated average values of factor \bar{M} for certain regions, i.e. for the weld filler metal and root weld metal of homogeneous and heterogeneous under-matched welds, which also confirms the validity of the experimental equation ($R_p = 3.15 \text{ HV} - 168$) [1] for yield strength calculation from the measured micro-hardness values in a welded joint.

4 CONCLUSIONS

In multi-pass under-matching joints with homogeneous and heterogeneous welds, a local strength mismatching, apart from the global strength mismatching ($M = \bar{R}_{pWM} / \bar{R}_{pBM}$), is also present. Local strength mismatching was determined by measurements of micro-hardness and is most prominent in the direction of thickness.

Local strength mismatching is caused by weld metal alloying and has a significant influence on fracture behaviour of weld metal regions with low toughness.

The homogeneous weld metal is due to an overmatched root still sensitive to cold cracking, which requires under-matched welds with a soft root layer and suitably chosen welding procedure, which takes into account a possibility of soft root layer alloying from the base material.

Acknowledgements

The authors wish to acknowledge the financial support of the Slovenian Foundation of Science and Technology and the Japanese Promotion of Science.

References

- [1] **Praunseis, Z.:** *The influence of Strength Under-matched Weld Metal containing Heterogeneous Regions on Fracture Properties of HSLA Steel Weld Joint* (Dissertation in English). Faculty of Mechanical Engineering, University of Maribor, Slovenia, 1998

- [2] **Praunseis, Z., Toyoda, M., Sundararajan, T.:** Fracture behaviours of fracture toughness testing specimens with metallurgical heterogeneity along crack front. *Steel res.*, Sept. 2000, 71, no. 9,
- [3] **Praunseis, Z., Sundararajan, T., Toyoda, M., Ohata, M.:** The influence of soft root on fracture behaviors of high-strength, low-alloyed (HSLA) steel weldments. *Mater. manuf. process.*, 2001, vol. 16, 2
- [4] **Sundararajan, T., Praunseis, Z.:** The effect of nitrogen-ion implantation on the corrosion resistance of titanium in comparison with oxygen- and argon-ion implantations. *Mater. technol.*, 2004, vol. 38, no. 1/2.

CAD MECHANISM SIMULATIONS VIA WEB ENVIRONMENTS

SIMULACIJE MEHANIZMOV CAD SISTEMOV NA SPLETU

Gorazd Hren[✉], Ivan Žagar

Keywords: CAD, Web services, mechanism simulation, VRML

Abstract

In the current competitive market and in the context of the complex development of products, designers must work as collaborative teams, involving customers throughout the design process. The globalization of industry is reflected in the need for collaborative work at remote locations; the internet provides the technologies for the communication necessary for such work. Designers are no longer exchanging only geometry, but more information about design knowledge and design solutions. In this paper, a framework is proposed for sharing simulations, including not only geometry and structural aspects but also behavioural criteria. The use of Java applets and an external authoring interface has been found suitable for that propose. The usage of standard web-based technologies leads to easier, more effective and more general applications suitable for small and medium-size companies with limited resources in the field of interactive visualisation of research. The proposed framework allows the automatic transfer of a mechanism defined by a CAD system into a web-based environment to investigate and evaluate solutions. The uniform application has been developed combining Java, XML and VRML on a Thin Client-Fat Server architecture. In order to avoid time-consuming virtual model preparation, product variety is defined in single XML file. The framework is an effective tool for engineering practice as well as for teaching and learning mechanism design and analysis.

[✉] Corresponding author: Gorazd Hren, Tel.: +386 7 620 2216, Fax: +386 7 620 2222, Mailing address: Fakulteta za energetiko, Hočevarjev trg 1, Krško, Slovenia
E-mail address: gorazd.hren@uni-mb.si

Povzetek

Pogoj za uspeh na konkurenčnem trgu in razvoj vedno bolj kompleksnih izdelkov, tako po geometriji kot izdelavi, je pogojen s sodelovanjem specializiranih strokovnjakov in vključevanje naročnika v celosten proces razvoja izdelka. Globalizacija industrije se odraža v potrebi po skupnem delu na oddaljenih lokacijah in internet ponuja tehnologijo za potrebno komunikacijo. Inženirji ne izmenjujejo le geometrijskih modelov, temveč vedno več informacij o inženirskih rešitvah in analizah teh rešitev. V tem prispevku je predstavljena spletna aplikacija, ki omogoča izmenjavo geometrije in strukture izdelka, pa tudi simulacije mehanizmov. Uporaba standardnih spletnih tehnologij vodi do razmeroma enostavnih, učinkovitih in splošnih rešitev, primernih za mala in srednje velika podjetja, ki imajo na tem področju raziskav omejene tehnološke in kadrovske vire. Razvita spletna aplikacija omogoča avtomatski prenos v CAD sistemu definirani mehanizem v spletno okolje za vrednotenje rešitve. Celostna rešitev vključuje Java programčke, XML in VRML na Thin Client - Fat Server arhitekturi. Aplikacija je učinkovito orodje za inženirsko izmenjavo in vrednotenje rešitev, kakor tudi za učenje in analize delovanja mehanizmov.

1 INTRODUCTION AND REVIEW

The design and development of complex mechanical systems is becoming a collaborative task among developing teams, which are usually geographically distributed. Because of the complexity of modern products, one designer can hardly manage the complete product development effort. Designers are no longer merely exchanging geometry data, but increasing amounts of design knowledge, specifications, partial solutions, assembly possibilities and functionalities. The computational frameworks supporting product engineering and collaboration in industry are becoming increasingly important.

Frequently, the evaluation of prototypes results in the modification of configurations; consequently, solutions or components are changed. The developed framework enables the cooperation of a broad set of participants in the production process, irrespective of tools used for modelling the product. The approach gives the opportunity for the interactive evaluation of products' behaviours from a prescribed set of components. The system is based on VRML (Virtual Reality Modelling Language), XML (eXtensible Mark-up Language) as configuration data carriers, and macro programming to automatically generate product in the CAD system. In this paper, the strategies used for achieving the integration of the CAD system and VRML and the Java user interface in order to develop interactive computer-modelled simulations of CAD-developed kinematic mechanisms are presented.

Leading CAD vendors (Dassault, UGS and PTC) have developed additional toolkits for visualizing assemblies as virtual prototypes directly from DMU or PDM. Recently, 3DVIA Composer was introduced for documentation exchange. The presentation and visualization quality of virtual prototypes is improving at an incredible rate. Since the user has no possibilities for manual interactions or influencing the quality of representation, the reviewing session is an automatic process and easily performed.

Particularly in engineering, the CAD model represents a fundamental model and the VR system is separated from CAD; the models are converted from CAD and enriched with additional information into a 3D virtual environment as a one-directional information flow; this makes it difficult to feedback modifications to CAD systems. For any change in the virtual environment, the changes have to be performed in CAD system, and converted again, because of consistency,

which leads to very unproductive and time-consuming repetitive loops. Integration is needed to improve the quality of evaluations and to reduce the time and work needed for modifications. Previous solutions are well presented by Zhang et al., [1]. The analyses of CAD models exchange possibilities are described in Gerbino et al., [2], benchmarking only geometry conversion from the system to system with and without healing tools, showing poor conversion results. Many researchers are using STEP for transferring data between applications. Coulibaly et al., [3], present a framework for behavioural performance with a generic object-oriented approach. The system is running separately from a CAD system (SolidWorks) using STEP and EXPRESS to translate a model from CAD and afterwards through work on mating condition recognition in the STEP file.

It has to be pointed out that virtual models in engineering are mainly tessellated CAD models, since a polygonal representation allows fast rendering in real time. Tessellation is conversion from the volume description of the object into surface descriptions with triangular patches; this method has some drawbacks: loss of object structure, model quality and redundant complexity. Typical problems in CAD-VR integration include the loss of geometric accuracy, assembly structure and data as dimensions, names, constraints, physical properties, etc. In order to achieve visualization and interaction, it is necessary to have a re-assignment of lost data in the conversion process, [4]. This extra work is inconvenient and consequently the use of VR technologies, in industry is used infrequently, especially in SMEs. The VR systems use a different dataflow for manipulating virtual models in real time; converting data into the VR format is maintained differently from system to system, greatly depending on the application. The work by Chouadria et al., [5], describes the simplification of the mesh models extracted from CAD systems as discrete models that can be easily used for visualization. The proposed approach is checking and maintaining the consistency of the assembly model. All activities are performed as middleware between the CAD system and the virtual environment in order to prepare models for manipulation of virtual mock-ups. The disadvantage, from an engineering point of view, is that the model is completely separated from the source.

When working on standard ways to share information over the web it is impossible to overlook XML. The XML specifications are publicly accessible and used in various research fields, as shown by Tao et al., [6], as an example from engineering domain. An increasing amount of research is preparing the virtual environment directly from PDM systems. Graf et al., [7], present a methodology to automate the processing of data preparation for the purposes of a design review in VR. The proposed system, VDDP, is directly integrated with the PDM and allows the user to navigate through the product structure, to correct geometric conversion errors and to reduce the complexity of the model. On the same topic, Jayaram et al., [8], present a method that improves the ability to use the virtual assembly environment to simulate real world assembly sequences in complex models, with differences between the sub-assembly and hierarchy representations in the CAD model and the component assembly sequence. In contrast, Xu et al., [9], propose a web-based virtual environment that allows designers from remote locations to cooperate in the same assembly scenario. The multimodal interaction and task processing are the basic technologies. Typically, the applications for kinematic simulation introduce toolkits with which the users should write the "simple programs" to solve complicated mechanism problems. The Mechanism Toolkit reported by Cheng et al., [10], is useful for analysing planar mechanisms and computing positions, velocities and accelerations for joints, and graphically representing the results. The toolkit is useful for learning purposes but rarely for real engineering product development, since all the analyses could be performed in the CAD system.

Many researches are using VRML as a sharing model or combine the VRML as a viewer with object-oriented programming languages to create VP. In van de Wetering, [11], a system using the combination of Java and VRML to handle the VRML scene graph and interactions with it using VRML prototype definitions is described. The combination of VRML and JavaScript creates a very strong tool for developing dynamic virtual worlds and on-line presentation of objects is presented in Qin et al., [12], while Cecil et al. [13] report on the integration from CAD to VRML only with adding definitions for translation and rotation into the VRML file directly; such information is unusable for other proposes.

The implementation of applications shows some drawbacks: the programming language is procedural and VRML is event driven, so the combination has to be very balanced to take advantages from both.

The combination of VRML, XML and Java technologies is used in many research works. Li, [14], described the optimization of distributed planning process to support product design and development. The system performs many computations to find surfaces and maintain assemblies to provide sequencing the machining operations. The integration of VRML and Java provides a standardized, portable and platform independent way to render interactive scenes via the web. The Web3D Consortium, [15], explained the possibilities of merging the two technologies, especially action sensors, interpolators, prototypes and scripting.

The idea of using macro files to retrieve an object is known from different applications, mostly databases and editors. The macro files in CAD systems contain the history of user commands during modelling process, generally used to avoid repetitive tasks with the definition of parameters. The use of macro files in CAD is described in the research of Choi et al., [16], and Mun et al., [17], where the interface captures modelling commands from macro file of one CAD system and transfers it into the macro file for the other CAD system. The interface works only for modelling a part, not assemblies. Since the modelling process varies from designer to designer, and the different CAD systems vary in their design algorithms, the conversion needs formalization.

As stated by Cera, [18], the research in collaborative design could be grouped into two categories: data-centric and interaction-centric. Virtual environments are developed for real-time interactions using static geometry data and not synchronously by multiple users. A trend in web applications shows the need for an ability to preview the product and (if possible) to investigate or test its functional behaviour. In the engineering domain, visualization support is frequently essential for evaluation. 3D virtual presentation of a product is a major step towards forming a truly convincing preview, leading to several technical and integration issues in the production process. Bettig et al., [19], report on a study for integrating different CAx modules into single framework combining scene-graphs and information models. They propose a new object based on well-defined paths to in CAx-generated data with problems on object presentation when using assemblies. Code development time is minimized by making as much use as possible of publicly and commercially available software (usually via API), but an interface must still be programmed to introduce the API to the rest of the program. Developers of custom CAD applications limit their development expenditures by not duplicating common functionalities already available in CAD packages, instead focusing on developing new functionalities. The downside of this approach is that many versions of the custom CAD applications must be developed, one for each CAD package to which the functionality will be added.

2 FEATURES OF WEB-BASED ENVIRONMENTS

In order to share the product design solutions, a great deal of manual work to transfer the kinematic simulation into a virtual environment is needed. This paper describes the on-going research on the architecture of the application addressing the sharing of VPs over the web with standard programming tools. The proposed approach enables the cooperation of a broad set of participants in the production process, irrespective of the tools used for modelling the product.

In the research, the focus is on the automatic generation of kinematic simulation from the CAD system into VRML for web-based distributed environments. The main issue is that the process automatically generates kinematic simulations for web services and no additional knowledge or work is needed to perform simulations. To investigate and evaluate more than one solution for the same function, the process is simple enough that the visualization pre-processing is a straightforward task. The web-based framework provides a convenient platform for users to view and evaluate a design model. A distributed design system can generate design models in an XML-style feature representation to allow a web-based system to perform viewing and manipulation, primarily in two main features:

- Taking advantages of the effective utilizations of the web and Java technologies makes the system independent of the operating system, scalable and service-oriented.
- The services located on the internet provide an accessible way for a designer to conduct the development process.

An XML-style representation has been used to carry out some features for visualization and manipulation in the web-based system. This format incorporates the characteristics of VRML and features to support web applications. The representation of XML-based information enables the system to be effectively adaptable to new developments of internet technology.

The system and services are based on the Java-Servlet mechanism. With the development of some new internet integration technologies, such as web services, it is necessary to explore new alternatives to integrate the current functions under the new system infrastructure. The system is organized as databases of files. The structure of the product and all links are defined in a configuration file using XML; VRML is used for viewing the VPs. In CAD systems, models are defined with features, and relations between parts are motion driven (using DOF). In the VRML models, in contrast to CAD assemblies, the constraints are generally performed by geometric calculation and sensors and motions are correspondingly time-defined or event-driven.

3 KINEMATIC SIMULATION OF MECHANISMS

There is a crucial need for suitable product models for efficient evaluation tools that allow behavioural performance assessment. The proposed framework has been developed to model a mechanical product including functional and structural aspects and behavioural criteria. In this chapter, the technologies used are briefly described, focusing on area of research.

3.1 Kinematic simulation of mechanisms in CAD

The CAD systems design environment provides much more information about design that is used for further analysis of the design solution. Functional behaviour in CAD systems is performed with kinematic simulations and analyses. The structural model of assembly is derived from functional specifications, by matching functions or constraints between related parts or sub-assemblies. In mechanical systems, several functions may be realised by the same set of parts or by the same sub-assemblies, or the same function could be performed by different set of parts or sub-assemblies.

In CAD, the kinematic analyses simulate the motion of mechanisms with mouse-based manipulation, and analyses it by checking interferences and computing minimal distances. The main task is to satisfy all degrees of freedom (DOF) for all parts of the product. There are two ways to generate the mechanism: using a wide variety of joints in a list or generating mechanisms automatically from defined assembly constraints. Automatically generated mechanisms depend crucially on accurate definitions of assembly constraints. The product assembly is rarely fully constrained, since not all DOF are constrained in the assembly process (e.g. rotation of bolts, nuts, pins where only the position and orientation is specified). Conflicts can arise between kinematic joint definitions and the assembly mating conditions. In our work, one important feature is that CAD allows the automation of mechanism creation and simulation through macro programming.

The creation of mechanism in CAD can be described with following steps:

- Define parts and sub-assemblies into product.
- Define the name of the mechanism and one grounded part to define the basic position of the entire mechanism.
- Define joints; the mechanism is ready for analysis when all the joints are defined.
- Analyse the mechanism that is a review of the mechanism's properties; it displays the number of DOF and free DOF.
- Define commands in joints according to the type of the joint (not all joints have commands). The mechanism has to have as many commands as there are free DOF in order to be able to simulate movement.
- Simulation, analysis and evaluation of the mechanism.

Simulation shows where all of the parts in an assembly are in time as it goes through a cycle. This technology is useful for simulating motion as well as in evaluating motions for interference purposes, such as the assembly sequences of complex assemblies. The forward kinematics are used, defining the motion of all joints that are explicitly specified. Animations of motion are the classic output from a simple kinematic analysis. The first use of such an animation is a simple visual evaluation of motion for the designer to see if it functions as desired. More sophisticated animations can be created to show motion from critical angles or even looking inside of parts, which is a significant advantage over building and running a physical prototype.

3.2 Simulation of mechanisms in VRML

The conjunction of VRML and Java with a custom communication protocol is one of the most important features of developing animations in virtual environment. Java is a platform-

independent, object-oriented programming language that can be used to control the movements in a virtual world (using any animation technique) and to construct user interfaces. Real-time presentation of animations with limited rendering quality is performed by efficient VRML browsers that are cost free and easy to obtain.

The paradigm to produce VRML scenes is based on nodes defining a scene graph. Each node is defined with a name, a type and parameters. There are two kinds of parameters: fields and events. Events can be sent from a node to another node by an *eventOut* parameter and received by an *eventIn* parameter that must be of the same type. Events process changes by external actions and can be propagated by the nodes using routing mechanism. Events and routes drive the animation in the virtual world. There are many kinds of nodes: geometric (define geometry of the object), grouping nodes (exhibit common behaviour and define the hierarchical structure) and particularly sensor and interpolator nodes. Sensor nodes generate events based on user interactions.

TouchSensor generates *eventOut* when the mouse is clicked or is over specified object. *TimeSensor* automatically generates an event with the animation clock. Interpolator nodes define the key-frames of an animation, interpolated by a linear function. As an example, the *PositionInterpolator* node defines n key positions in n associated time instants. Routing the *TimeSensor* to *PositionInterpolator* generates an event at each time fragment, representing the current position from interpolation function. The same mechanism is used with *OrientationInterpolator* to define the orientation of the object in time. A typical use is defined with *TouchSensor* routed to *TimeSensor* that starts the clock with the mouse click. The *TimeSensor* is routed to *PositionInterpolator* or *OrientationInterpolator* or both, sending time values for the interpolation function. The interpolator is linked to a geometric node, changing the position, orientation or both of the objects. Since the routing mechanism is limited with logical operations, the *Script* node allows the user to connect the simulation to a program, where the events can be processed. Direct interaction with the user is performed via sensors, interpolators and scripts.

3.3 XML

In this approach, XML is used as a dynamic language for the structured representation of data with defined tags. The robust extensibility of XML makes it a perfect fit for a hierarchical, semantically embedded representation of data. XML has many advantages over other data formats: it is simple, easy to use, license free, platform independent, well-supported, and follows international standards. Another strong point of XML is the availability of parsers that are license free. The syntax and structure must be checked to insure integrity and data type validity, which is performed by the XML parser.

4 IMPLEMENTATION

The web-based framework provides a convenient platform for users to view and evaluate a design model. A distributed design system can generate design models in an XML-style feature representation to allow a web-based system to perform viewing and manipulation, with two main features:

- By taking advantages of the effective utilizations of the Web and Java technologies, this system is independent of the operating system, scalable and service-oriented. The services located in the internet can provide an effective manner for a designer to conduct development process.
- A new XML-style representation has been used to carry out some features for visualisation and manipulation in the web-based system. This format incorporates the characteristics of VRML and features to support Web applications. The XML-based information representation enables the system to be effectively adaptable to meet new developments of internet technology.

The current system and services are based on the Java Servlet mechanism. With the development of some new internet integration technologies, such as web services, it is necessary to explore new alternatives to integrate the current functions under the new system infrastructure. A schematic of the framework is presented in Figure 1.

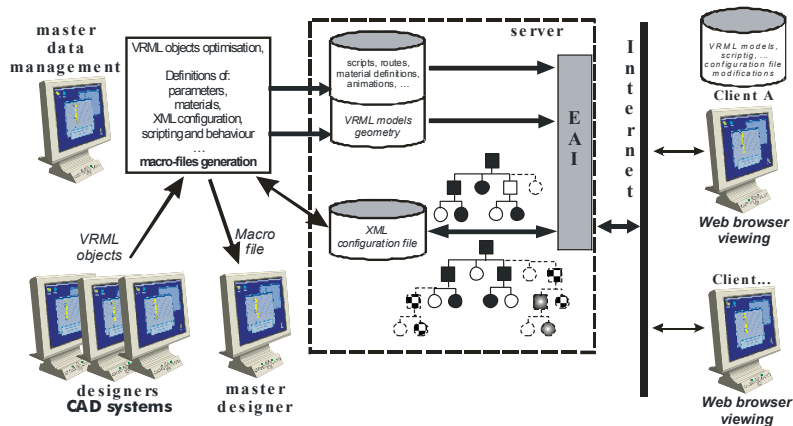


Figure 1: System architecture.

It has to be pointed out that the configuration file is generated only for the first main assembly. For alternate sub-assemblies or parts, all actions are performed but configuration file, which is supplemented with additional and alternate objects. Information on appearance, sensors, interpolators, scripts and routing parameters for object functionality and dynamic behaviour definitions is added and can be interactively controlled by the user. These preparations were first done manually with much tedious and time-consuming work; but when all objects and scripts are prepared, the task is not so complicated if the rules and definitions are followed. Recently, an editor has been developed that allows changing the configuration more effectively and interactively. Finally, the extended database consists of geometry and material appearances of parts, additional definitions and the configuration file that links the structure of the assembly with attributes. The output of the editor can be seen in Figure 2. The editor enables changing and adding different parameters into the configuration file. The configuration objects is shown as tree in which the selected options are indicated with different colours.

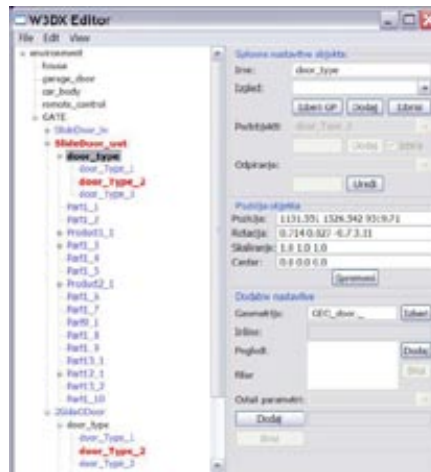


Figure 2: The editor outlook.

Selecting the element (a sub-assembly or part), the parameters are presented in the manipulation window, divided into three major parts:

- general properties:
 - name of the element
 - appearance (selecting from defined appearances or define new one with all parameters, e.g. colour, transparency, texture definition)
 - all sub-elements are listed (adding or removing elements)
 - adding or changing the global parameters
- geometrical position of the element (transformation, rotation, scaling and centre) needed for VRML sensors):
- additional options with definition of which element:
 - name of the file with geometry or the element could be added using Inline definition (URL),
 - adding different views if needed (name of the file with the view definition),
 - additional parameters as sensors and routes defined in files.

It is possible to check the outlook anytime with the view option in a separate window with a VRML browser so the preparation process is the subject of the instant evaluation. The editor has replaced a great deal of previous manual work needed for preparing the configuration file with several options.

The following section describes the testing of the framework on a real example. The aim of the implementation in engineering is to test different solutions. In mechanical engineering, the detail geometry is an important matter. Figure 3 is an example of a remote-controlled gate solution with a problem of limited space. Three solutions were implemented; two with slide gates (inside and outside) and one with the opening of each half of the gate. All parts and assemblies were modelled with CAD. For first solution, the macro program generated the configuration file, gate geometry and appearance files with assembly constraints. The alternative solutions were modelled and extracted separately and afterwards added to the structure using the editor. The house, remote control device and car were included in the configuration file and positioned with the editor as *Inline* node. To simulate the behaviour,

sensors and scripts nodes are linked to remotely control the opening of the gate. The very detailed solution is geometrically complicated and found to be almost inappropriate for applications working over the web; an extensive amount of data was needed. The speed and response of the application is sensitive to local computer performance.

In Figure 3, the outlook of the framework is presented. In the left window, the user has to log-in and select the name of the configuration file to get the structure. After the *VISUALISE* button is selected, the server generates the VRML file from the configuration file and displays it in the view window. The user can navigate the space and use interactive possibilities of the browser to open and close the gate. The user can easily select one of the three given choices of opening the gate as main solutions, and three types of the gate to investigate the behaviour of the selected one. In the framework, the user has the possibility to add an object into the configuration file as an alternative to the existing objects or to write the comment to the master user. In Figure 4, the fractions of the configuration file for the discussed example is presented. All main functions are shown: clear hierarchical structure, choice definition and including the elements from remote location (inline).

The selected configuration is saved in user folder with time and user name as a selected version. The different options could be shown to the customer on remote location and the accepted solution can be forwarded directly to the CAD system. The master designer has the authority to run the macro program in the CAD system to rebuild assembly from the configuration file. The next step is to generate all documentation (drawings) and bill of material for production purpose that is automatically obtained from the CAD system. This example demonstrates the effectiveness and usability of the framework in collaborative work using the web.

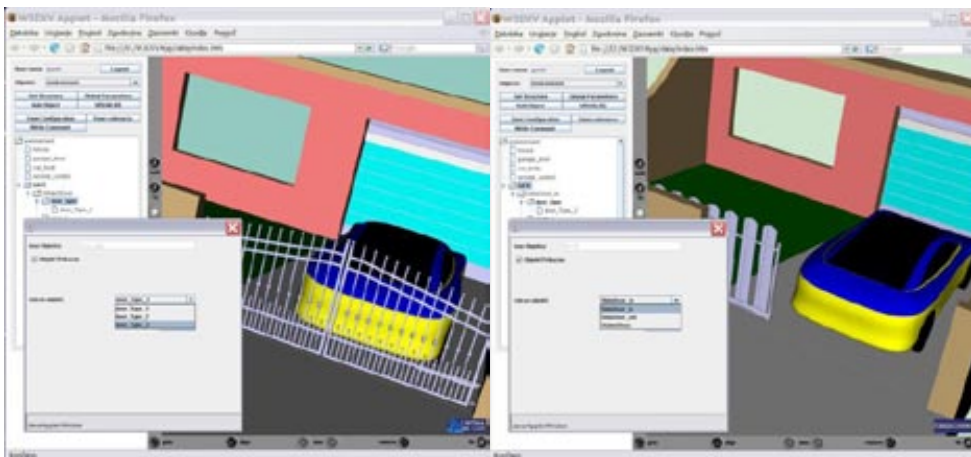


Figure 3. The application outlook when using different choices.

```

-----
<object ime="complete" BG="Background._">
  <object ime="house" inline="http://?/house.wrl"/>
  <object ime="garage_door" inline="http://?/garage_door.wrl">
    <poz>...</poz>
  </object>
  <object ime="car_body" inline="http://?/vrml/car.wrl">
    <poz>...</poz>
  </object>
  <object ime="remote_control" inline="http://?/vrml/remoteC.wrl">>
    <poz>...</poz>
  </object>
  <object choice="0" ime="GATE">
    <object ime="SlideDoor_in" ROUTE="SlideDoor._">
      <poz>...</poz>
      <object ime="door_type" choice="2">
... ..
        </object>
... ..
    <object ime="SlideDoor_out" ROUTE="SlideDoor._">
      <poz>...</poz>
      <object ime="door_type" choice="1">
        <object ime="door_Type_1" GEO="GEO_dT1._" ROUTE="R_door._"/>
        <object ime="door_Type_2" GEO="GEO_dT2._" ROUTE="R_door._"/>
        <object ime="door_Type_3">
          <object ime="dT3_left" GEO="GEO_dT3._" ROUTE="R_dT3Left._"/>
          <object ime="dT3_right" GEO="GEO_dT3._" ROUTE="R_dT3Right._"/>
        </object>
      </object>
... ..
    <object ime="2Side0Door" ROUTE="2Side0Door._" >
      <object ime="door_type" choice="2">
... ..
        </object>
... ..
      </object>
... ..
    </object>
... ..
  </object>
</object>

```

Figure 4: The fragments of configuration file.

5 CONCLUSIONS

The collaborative design chain includes the customer, designers, manufacturers and suppliers for specific partial solutions. The concurrent methodology can be implemented when internet-based technologies link all participants with continuous data and information exchange at remote locations.

In contrast to an expensive physical prototype for the product design and performance verification, the virtual prototype offers evaluation in the digital world. The digital mock-up is not just for a graphic visualization of the assembly, but also includes the behaviour of response to user's interactions.

In engineering, the visualisation is of crucial importance. Usage of standard web technologies leads to easier, effective and more general applications. In the presented approach, the VRML is used for sharing models over the web using XML as a structured data carrier and integrator. The framework enables the generation of VP for viewing and evaluation of the functionality in a

standard VRML browser. We have to consider the consistency of databases, which is ensured since the programs perform almost no arithmetical operations. To implement X3D would be a logical choice, since the X3D standard uses XML syntax, which provides synergy and will substitute for the VRML. VRML models will be replaced by X3D models when the converters will be available directly in the CAD systems.

The framework is cost effective since the required infrastructure exists and the viewing software is available. Current limitations are dictated by network capabilities (download times for large VRML files describing complex virtual models) and the speed of the user's local computer (responsible for real-time rendering and interactions). This approach presents a solution of virtual prototype exchange over the web using a standard freeware tool that makes it very suitable for SMEs with limited resources.

References

- [1] **S Zhang, W Shen, H Ghenniwa.** (2004) *A review of Internet-based product information sharing and visualization*. Computers in Industry; 54, pp.1–15
- [2] **C Gerbino, A Brondi.** (2004) *Interoperability issues among CAD systems: a benchmarking study of 7 commercial MACD software*. Proc DESIGN 2004; pp.457–464
- [3] **A Coulibaly, B Mutel, D Ait-Kadi.** (2007) *Product modeling framework for behavioral performance evaluation at design stage*, Computers in Industry; 58, pp.567–577
- [4] **WC Regli, VA Cicirello.** (2000) *Managing digital libraries for computer-aided design*. Computer-Aided Design; 32, pp. 119–132
- [5] **R Chouadria, P Veron.** (2006) *Identifying and re-meshing contact interfaces in a polyhedral assembly for digital mock-up*. Engineering with Computers; 22, pp.47–58
- [6] **YH Tao, TP Hong, SI Sun.** (2004) *An XML implementation process model for enterprise applications*. Computers in Industry; 55, pp.181–196
- [7] **H Graf, G Brunetti, A Stork.** (2002) *A methodology supporting the preparation on 3D-CAD data for design reviews in VR*. Proc DESIGN 2002; pp.489–495
- [8] **U Jayaram, Y Kim, S Jayaram, VK Jandhyala, T Mitsui.** (2004) *Reorganizing CAD assembly models (as-Designed) for manufacturing simulations and planning (as-Built)*. Journal of Computing and Information Science and Engineering; 4, pp.98–108
- [9] **Y Xu, X Meng, W Liu, H Xiang.** (2006) *A collaborative virtual environment for real time assembly design*. Virtual reality continuum and its applications, Proc ACM international conference on Virtual reality continuum and its applications 2006; 2, pp.373–376
- [10] **Cheng HH, Trang DT.** (2006) *Object-oriented interactive mechanism design and analysis*. Engineering With Computers; 21, pp.237–246
- [11] **H van de Wetering.** (2001) *Javra: a simple, extensible Java package for VRML*. Proc Computer Graphics International 2001; 333–336
- [12] **SF Qin, R Harrison, AA West, DK Wright.** (2004) *Development of a novel 3D simulation modeling system for distributed manufacturing*. Computer-Aided Design, 36, pp.761–773

- [13] **J Cecil, A Kanchanapiboon.** (2007) *Virtual engineering approaches in product and process design*. International Journal of Advanced Manufacturing Technology; 31, pp.846–856
- [14] **WD Li.** (2005) *A Web-based service for distributed process planning optimization*, Computers in Industry; 56, pp.272–288
- [15] **D Brutzman.** *The Virtual Reality Modeling Language and Java*, Communications of the ACM 1998; 41(6):57–64
- [16] **GH Choi, D Mun, S Han.** (2002) *Exchange of CAD Part Models Based on the Macro-Parametric Approach*. International Journal of CAD/CAM; 2, pp.23–31
- [17] **D Mun, S Han, J Kim, Y Oh.** (2003) *A set of standard modeling commands for the history-based Parametric Approach*. Computer-Aided Design; 35, pp.1171–1179
- [18] **CD Cera, T Kim, J Han, WC Regli.** (2004) *Role-based viewing envelopes for information protection in collaborative modelling*. Computer-Aided Design; 36(9), pp.873–886
- [19] **B Bettig, V Bapat.** (2006) *Integrating multiple information presentations in a single CAD/CAM/CAE environment*. Engineering with Computers; 22, pp.11–23

NUMERICAL EVALUATION OF THE CRACK-DRIVING FORCE IN HETEROGENEOUS REGIONS

NUMERIČNA DOLOČITEV SILE RAZVOJA RAZPOKE V HETEROGENIH PODROČJIH

Zdravko Praunseis[✉]

Keywords: crack-driving force, numerical simulation, crack tip

Abstract

An attempt to evaluate numerically the crack-driving force CTOD - δ_5 for welded joints with a strength mismatch has been made with use of the finite element method. The crack-driving force, i.e. the parameter CTOD - δ_5 , for specimens with shallow cracks in welded joints with homogeneous and heterogeneous welds, has been determined at the point of instability. Different yield strengths of different microstructures around the crack tip and its actual mechanical properties are taken into account in the finite element method model of bending specimens. The idea of the numerical evaluation of the CTOD - δ_5 parameter is to evaluate the crack-driving force and to compare it with the experimental value in order to estimate if brittle or ductile fractures will be initiated.

Povzetek

Obravnavana je numerična določitev sile razvoja razpoke CTOD - δ_5 s pomočjo metode končnih elementov za trdnostno neenake zvarne spoje. Za preizkušance s plitvimi razpokami v homogenem in heterogenem zvarnem spoju je dočena sila razvoja rapoke v trenutku nestabilnosti, t.j. parameter CTOD - δ_5 . Pri numeričnem modeliranju upogibnega preizkušanca z metodo končnih elementov so upoštevane v okolici konice razpoke različne meje tečenja pojavnih mikrostruktur in njene dejanske mehanske lastnosti. Namen numerične določitve

[✉] Corresponding author: Zdravko Praunseis, PhD, Faculty of Energy Technology, University of Maribor, Tel.: +386 31 743 753, Fax: +386 7 620 2222, Mailing address: Hočevarjev trg 1, Krško, Slovenia, E-mail address: zdravko.praunseis@uni-mb.si

parametra CTOD - δ_5 je v določitvi sile razvoja rapoke in v primerjavi z eksperimentalnimi vrednostmi ter ocenitvi pojava iniciacije krhkega ali žilavega loma.

1 INTRODUCTION

The aim of the finite element method (FEM) analysis was to evaluate the crack-driving force - δ_{5MKE} numerically on one type of bend specimens $B \times B$ with and without a soft root layer, as well as to evaluate the fracture behaviour of regions around the crack tip with different strength mismatches. If it turns out that the numerical driving force values are comparable with the experimental values of fracture toughness ($\delta_{5(i/c)}$), then the load at brittle or ductile fracture initiation can be predicted on the basis of the calculated crack-driving force. A fracture (brittle or ductile) will initiate at point T_N , where the driving force acts as a tangent to the CTOD - δ_5 resistance curve as shown in Figure 1, [1–4].

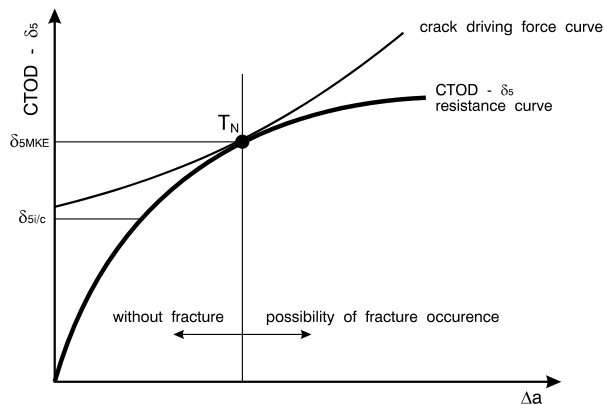


Figure 1: Evaluation of instability point

For fractures to occur at the point T_N it is necessary that the driving force - δ_{5MKE} equals the material resistance parameter, i.e. the experimentally evaluated fracture toughness - $\delta_{5(i/c)}$. With the numerical modelling of the welded joints, it was intended to obtain the size and the shape of the plastic zone at the crack tip at the moment of brittle or ductile fracture initiation in specimens with plane stress conditions at the crack tip.

2 NUMERICAL MODELLING OF WELDED JOINT

The numerical analysis was done for bend specimens ($B \times B$, $B = 36$ mm) with shallow cracks in homogeneous and heterogeneous welds [1–2]. For the analysis, the homogeneous (Fig. 2a) and heterogeneous welds (Fig. 2b) were simplified regarding the geometry and material, e.g. the fusion line between the weld metal and the heat affected zone (HAZ) was taken as a straight line, and multi-pass welding (built up) was not taken into account. Due to the symmetry of bending specimen $B \times B$ (Fig. 3), only one half of the specimen was modelled. Characteristic points for δ_5 measurement were marked on the specimen surface for CTOD testing.

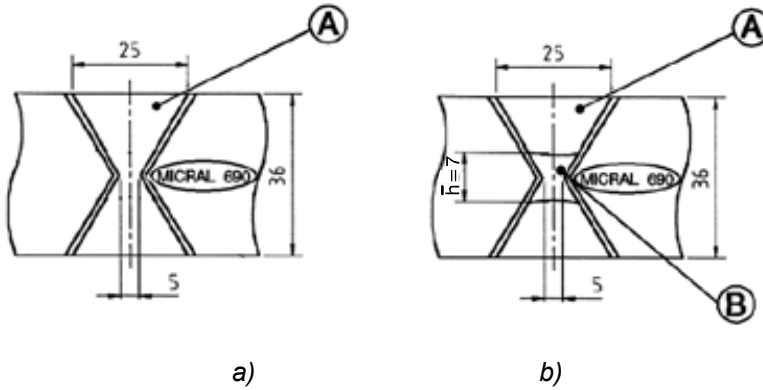


Figure 2: Geometry of homogeneous a) and heterogeneous b) weld joints

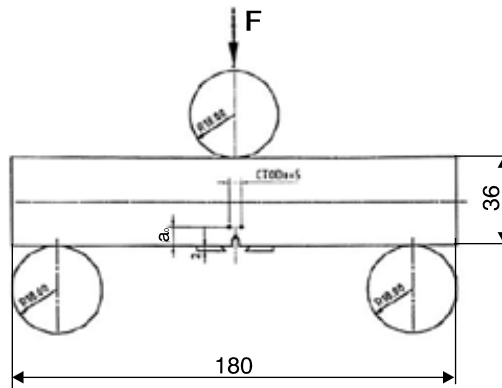


Figure 3: Geometry of bend specimen $B \times B$ with shallow crack and the position of characteristic points for δ_5 measurement

For the numerical modelling of bend specimen $B \times B$ with a shallow crack in homogeneous and heterogeneous welds, the two-dimensional finite element mesh, as shown in Fig. 4, was used. The specimen was loaded in the plane of symmetry in direction of the positive y -axis. Displacement in the y -direction was constrained at the specimen support node. Displacements in the x -direction were constrained along the specimen ligament.

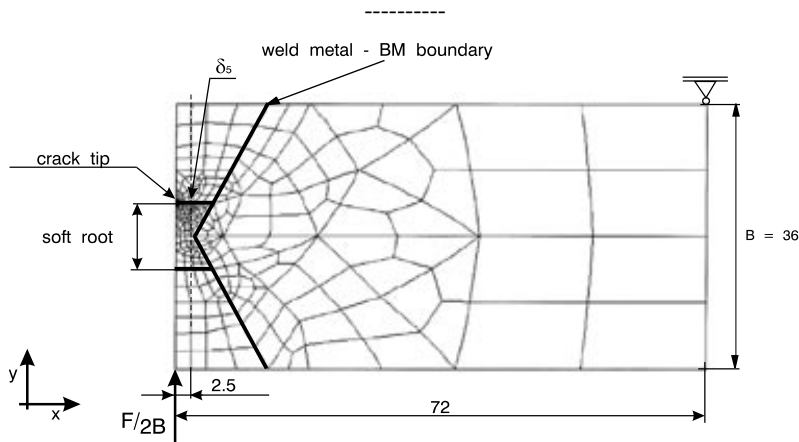


Figure 4: Finite element mesh for bend specimen $B \times B$ with shallow crack in homogeneous and heterogeneous welds

In order to lower the effect of plastic strains in support (at symmetry axis) and the effect of strain on loading simulation of SENB specimens, the force $F/2$ in the support was distributed along the specimen thickness B . For CTOD - δ_5 evaluation, the mesh was generated with the crack tip node horizontally distanced 2.5 mm from the specimen symmetry line. Finite crack sharpness was simulated by circle $r = 0.02$ mm, as shown by the detail of the mesh in the crack tip vicinity in Fig. 4. This is scaled with initial sharpness of the fatigue crack tip, [2], prepared as a standard specimen, [1]. FEM analysis, [1], has shown that the crack tip sharpness up to $r = 0.1$ mm did not influence the plastic zone size in the moment of initial fracture, which is five times larger than crack tip sharpness $r = 0.02$ mm used in this investigation. Because the finite crack tip sharpness was used, special finite elements were not needed. Isoparametric eight-noded finite elements were used for the mesh. The FEM analysis was used to estimate the influence of the soft root layer B with lower yield strength ($R_p \sim 600$ MPa) and width $h = 7$ mm on the crack-driving force value CTOD - δ_5 and thus on the size and shape of strain-hardening zone at the crack tip in the moment of fracture initiation (brittle or ductile). For numerical modelling, a $B \times B$ one specimen with shallow cracks in the homogeneous weld and two specimens with shallow cracks in the heterogeneous weld were used.

Uniaxial stress-strain behaviour ($\sigma - \varepsilon$ diagram) of materials A, B and MICRAL 690 for FEM modelling was modelled with the linear Hooke law up to the yield point, and in the strain hardening region with the Ludwik potential equation ($\sigma = A \varepsilon^n$), [1], regarding the calculated mechanical properties from Table 1, as shown in Figure 5.

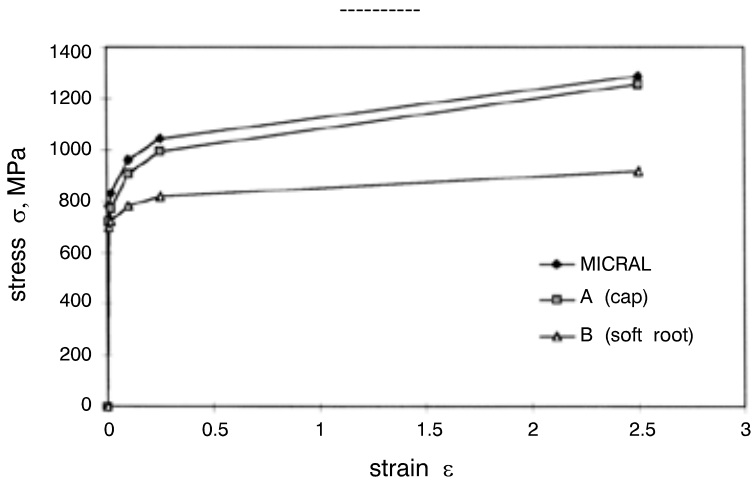


Figure 5: Piecewise linear curves for uniaxial stress-strain FEM modelling of material A (WELTEC B 575), B (WELTEC B 370) and MICRAL 690

The values for n (strain hardening coefficient), A (strength coefficient), σ_m (tensile strength), ϵ_m (tensile strain), σ_f (fracture stress) and ϵ_f (fracture strain) were calculated by using the experimental true ($\sigma - \epsilon$) curves for materials A, B and MICRAL 690, given in Table 1.

Table 1: Mechanical properties calculated by using experimental true ($\sigma - \epsilon$) curves of materials A, B and MICRAL 690

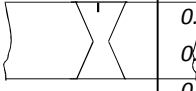
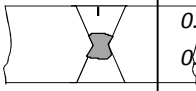
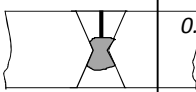
Value	MICRAL 690	A (weld metal)	B (soft root)
n	0.09068	0.10109	0.04980
A [MPa]	1183.5	1143.8	876
σ_m [MPa]	909	871	757
ϵ_m	0.05332	0.06555	0.0572
σ_f [MPa]	1497	1530	1330
ϵ_f	1.010	0.95	1.175

For the FEM analysis, the software system ABAQUES was used. Simulation of SENB specimen loading was done with gradual increase of force increments F and calculation of appropriate δ_5 values at each load increment. The stiffness matrix was calculated for every load increment. The system of equations was solved with the Newton-Raphson method [A 4.26] and the Von Mises yield criterion was employed [3]. For strains and strain energy, and residual forces the tolerance criterion was set to 0.1%.

3 RESULTS AND DISCUSSION

Numerical values of driving force CTOD - δ_5 for B x B specimens with shallow cracks in homogeneous and heterogeneous welds, together with experimental values CTOD - δ_5 are given in Table 2.

Table 2: Results of experimental CTOD - δ_5 fracture toughness and numerical driving force - δ_{5MKE} values for specimens B x B with shallow crack in homogeneous and heterogeneous welds

Specimen B X B	δ_i [mm]	$\delta_{0.2}$ [mm]	δ_c [mm]	δ_u [mm]	a/W _{EKS}	δ_{5MKE}	a/W _{MKE}
	0.117	0.191		0.336	0.227	0.106	0.25
	0.100	0.175		0.325	0.239		
	0.103	0.162		0.256	0.261		
	0.089	0.108		0.169	0.255		
	0.089	0.140		0.148	0.327	0.079	0.34
	0.071		0.111	0.346			
	0.062		0.097	0.376			
			0.076	0.350			
	0.037		0.042		0.394	0.036	0.40
			0.044		0.381		
			0.034		0.401		
			0.032		0.423		

The relationship between the strain value at the crack tip and the fracture strain has been chosen as the criterion for material de-cohesion in simulations of the SENB specimen loading. It has been assumed that fracture initiates (either brittle or ductile) at the moment the strain value at the crack tip reaches the fracture strain.

Discrepancies between the numerical and experimental curves F - CTOD, as well as between the experimental results of fracture toughness $\delta_{5i/c}$ and the numerical values of the crack-driving force δ_{5FEM} are due to the following reasons:

- The role of the hardening exponent n in homogeneous and heterogeneous welds is not entirely clear, because round tensile specimens were not taken exactly from the regions where the fatigue crack tip was positioned, and represent only the average mechanical properties of weld metal regions from which they have been extracted. In this example, the hardening exponent n was overestimated, producing higher numerical values of the crack-driving force δ_{5FEM} , since the fracture strain values were overrated. In contrast, the conservative values of hardening exponent n resulted in the underestimated fracture strain, producing lower values for the crack-driving force δ_{5FEM} .

-
- The real mechanical properties of homogeneous and heterogeneous welds, used for numerical simulation of SENB specimen loading, were obtained at room temperature, while the real CTOD values were obtained at $-10\text{ }^{\circ}\text{C}$, which is also one of the reasons for the overestimated n values, which had the effect of increasing the crack-driving force δ_{FEM} . It is well known that the yield and tensile strengths increase with decreases of the temperature, because of ductility, i.e. fracture strain.
 - The effect of the microstructure on CTOD values was more pronounced in the set of specimens with crack depth $a/W \sim 0.40$ and fatigue crack tip position at the soft root layer boundary, since the microstructure at crack tip changed considerably with a small increase of crack depth: a/W . Specifically, variable soft root layer thickness, which was a consequence of soft root layer built up (welding), did not prevent the fatigue crack tip positioning exactly at the soft root layer boundary in either specimen.
 - A lower degree of plastic flow was achieved in specimens with homogeneous welds than in specimens with heterogeneous welds, due to the higher hardening degree (higher n) of homogeneous welds. This was mainly due to the higher 'average loading capacity' of homogeneous welds in comparison to heterogeneous welds. The homogeneous weld was made by the same consumable (WELTEC B 575) and had a higher average hardening capability compared to heterogeneous weld, which was 'weakened' with the soft root layer (WELTEC B 370). In the SENB specimen with the crack tip position at the soft root layer boundary, the brittle fracture has initiated when the material flow contour crossed the fusion line. Soon after the specimen loading started, it failed in a brittle manner, due to higher strain ability (lower n) and lower hardening capability of soft root layer, thus disabling plastic strains in the base material and under-matched weld metal.

4 CONCLUSIONS

Good agreement between calculated (δ_{BS}) and measured (δ_5) CTOD values is obvious from the comparison of CTOD results, verifying the method of direct measurement of CTOD, for which the material property data (e.g. yield strength) is not necessary, contrary to the calculated CTOD values according to the standard BS 5762. This argument favours using direct measurement δ_5 at crack tip in welded joints with local and global strength mismatching and precludes the application of the BS 5762 standard for welded joints, which is valid for base material.

Relatively good approximation of the experimental results by the numerical simulation of crack-driving force CTOD- δ_5 indicates the possibility of using FEM for evaluation of the crack initiation driving force for mismatched welded joints.

Acknowledgements

The authors wish to acknowledge the financial support of the Slovenian Foundation of Science and Technology and the Japanese Promotion of Science.

References

- [1] **Praunseis, Z.:** *The influence of Strength Under-matched Weld Metal containing Heterogeneous Regions on Fracture Properties of HSLA Steel Weld Joint* (Dissertation in English). Faculty of Mechanical Engineering, University of Maribor, Slovenia, 1998
- [2] **Praunseis, Z., Toyoda, M., Sundararajan, T.:** Fracture behaviours of fracture toughness testing specimens with metallurgical heterogeneity along crack front. *Steel res.*, Sep. 2000, 71, no. 9,
- [3] **Praunseis, Z., Sundararajan, T., Toyoda, M., Ohata, M.:** The influence of soft root on fracture behaviors of high-strength, low-alloyed (HSLA) steel weldments. *Mater. manuf. process.*, 2001, vol. 16, 2
- [4] **Sundararajan, T., Praunseis, Z.:** The effect of nitrogen-ion implantation on the corrosion resistance of titanium in comparison with oxygen- and argon-ion implantations. *Mater. tehnol.*, 2004, vol. 38, no. 1/2.

AUTHOR INSTRUCTIONS (MAIN TITLE)

SLOVENIAN TITLE

Authors, Corresponding author^{3†}

Key words: (Up to 10 keywords)

Abstract

Abstract should be up to 500 words long, with no pictures, photos, equations, tables, only text.

Povzetek

(In Slovenian language)

Submission of Manuscripts: All manuscripts must be submitted in English by e-mail to the editorial office at jet@uni-mb.si to ensure fast processing. Instructions for authors are also available online at www.fe.uni-mb.si/si/jet.html.

Preparation of manuscripts: Manuscripts must be typed in English in prescribed journal form (Word editor). A Word template is available at the Journal Home page.

A title page consists of the main title in the English and Slovenian languages; the author(s) name(s) as well as the address, affiliation, E-mail address, telephone and fax numbers of author(s). Corresponding author must be indicated.

Main title: should be centred and written with capital letters (ARIAL **bold** 18 pt), in first paragraph in English language, in second paragraph in Slovenian language.

Key words: A list of 3 up to 6 key words is essential for indexing purposes. (CALIBRI 10pt)

Abstract: Abstract should be up to 500 words long, with no pictures, photos, equations, tables, - text only.

Povzetek: - Abstract in Slovenian language.

^{3†} Corresponding author and other authors: Title, Name and Surname, Tel.: +XXX x xxx xxx, Fax: +XXX x xxx xxx, Mailing address: xxxxxxxxxxxxxxxxxxxxxxxxxxxxxxxxxxxx, E-mail address: email@xxx.xx

Main text should be structured logically in chapters, sections and sub-sections. Type of letters is Calibri, 10pt, full justified.

Units and abbreviations: Required are SI units. Abbreviations must be given in text when first mentioned.

Proofreading: The proof will be send by e-mail to the corresponding author, who is required to make their proof corrections on a print-out of the article in pdf format. The corresponding author is responsible to introduce corrections of data in the paper. The Editors are not responsible for damage or loss of manuscripts submitted. Contributors are advised to keep copies of their manuscript, illustrations and all other materials.

The statements, opinions and data contained in this publication are solely those of the individual authors and not of the publisher and the Editors. Neither the publisher nor the Editors can accept any legal responsibility for errors that could appear during the process.

Copyright: Submissions of a publication article implies transfer of the copyright from the author(s) to the publisher upon acceptance of the paper. Accepted papers become the permanent property of “Journal of Energy Technology”. All articles published in this journal are protected by copyright, which covers the exclusive rights to reproduce and distribute the article as well as all translation rights. No material can be published without written permission of the publisher.

Chapter examples:

1 MAIN CHAPTER

(Arial bold, 12pt, after paragraph 6pt space)

1.1 Section

(Arial bold, 11pt, after paragraph 6pt space)

1.1.1 Sub-section

(Arial bold, 10pt, after paragraph 6pt space)

Example of Equation (lined 2 cm from left margin, equation number in normal brackets (section.equation number), lined right margin, paragraph space 6pt before in after line):

$$c = \sqrt{a^2 + b^2} \tag{1.1}$$

Tables should have a legend that includes the title of the table at the top of the table. Each table should be cited in the text.

Table legend example:

Table 1: Name of the table (centred, on top of the table)

Figures and images should be labelled sequentially numbered (Arabic numbers) and cited in the text – Fig.1 or Figure 1. The legend should be below the image, picture, photo or drawing.

Figure legend example:

Figure 1: Name of the figure (centred, on bottom of image, photo, or drawing)

References

[1] **Name. Surname:** *Title*, Publisher, p.p., Year of Publication

Example of reference-1 citation: In text, Predin, [1], text continue. **(Reference number order!)**

SiPRO
INŽENIRING

Gen
ENERGIJA

JET

JET Journal of ENERGY TECHNOLOGY

Vol. 5/4 2012

UNIVERSITY OF MARIBOR, FACULTY OF ENERGY TECHNOLOGY



ISSN 1855-5748